T.R.
ONDOKUZ MAYIS UNIVERSITY
INSTITUTE OF GRADUATE STUDIES
DEPARTMENT OF ELECTRICAL AND ELECTRONICS ENGINEERING

MIMO ANTENNA DESIGN FOR 5G MILLIMETER-WAVE COMMUNICATION SYSTEMS

Master's Thesis

Nermin K.A. HAMDAN

Supervisor

Assoc. Prof. Dr. Çetin KURNAZ

SAMSUN
2023

ACCEPTANCE AND APPROVAL OF THE THESIS

The study entitled **"MIMO ANTENNA DESIGN FOR 5G MILLIMETER-WAVE COMMUNICATION SYSTEMS"** prepared by **Nermin K.A. HAMDAN**, and supervised by **Assoc. Prof. Dr. Çetin KURNAZ**, was found successful and unanimously accepted by committee members as Master thesis, following the examination on the date 12.1.2023.

	Title Name SURNAME **University** **Department/Art**	**Final Decision**
Chairman	Assoc. Prof. Dr. Hülya GÖKALP CLARKE Ondokuz Mayıs University Department of Electrical and Electronics Engineering, SAMSUN	☒ Accept ☐ Reject
Member	Assoc. Prof. Dr. Çetin KURNAZ Ondokuz Mayıs University Department of Electrical and Electronics Engineering, SAMSUN	☒ Accept ☐ Reject
Member	Assoc. Prof. Dr. Fatih KABURCUK Sivas Cumhuriyet University Department of Electrical and Electronics Engineering, SİVAS	☒ Accept ☐ Reject

This thesis has been approved by the committee members that already stated above and determined by the Institute Executive Board.

.

Prof. Dr. Ahmet TABAK
Head of Institute of Graduate Studies

DECLARATION OF COMPLIANCE WITH SCIENTIFIC ETHIC

I hereby declare and undertake that I complied with scientific ethics and academic rules in all stages of my Master's Thesis , that I have referred to each quotation that I use directly or indirectly in the study and that the works I have used consist of those shown in the sources, that it was written in accordance with the institute writing guide and that the situations stated in the article 3, section 9 of the Regulation for TÜBİTAK Research and Publication Ethics Board were not violated.

Is Ethics Committee Necessary?

Yes ☐ (If it necessary, please add appendices.)

No ☒

12 /01 / 2023
Nermin K.A. HAMDAN

DECLARATION OF THE THESIS STUDY ORIGINALITY REPORT

Thesis Title : MIMO ANTENNA DESIGN FOR 5G MILLIMETER-WAVE COMMUNICATION SYSTEMS

As a result of the originality report taken by me from the plagiarism detection program on 08 /12 /2022 for the thesis titled above;

Similarity ratio : % 15

Single resource rate : % 2 has been released.

12 /01 / 2023
Assoc. Prof. Dr. Çetin KURNAZ

ÖZET

5G MİLİMETRE DALGA HABERLEŞME SİSTEMLERİ İÇİN MIMO ANTEN TASARIMI

Nermin K.A. HAMDAN
Ondokuz Mayıs Üniversitesi
Lisansüstü Eğitim Enstitüsü
Elektrik-Elektronik Mühendisliği Ana Bilim Dalı
Yüksek Lisans, Ocak/2023
Danışman: Doç. Dr. Çetin KURNAZ

Haberleşme alanında sürekli iyileştirme gerektiren 5G anten tasarımı günümüzün popüler araştırma konularındandır. 5G sisteminde kanal kapasitesi mikroşerit MIMO anteni kullanılarak arttırılabilir. MIMO performans iyileştirmesi sağlamak için birden fazla anten kullanan bir teknolojidir. Mikroşerit anten, diğer anten türlerine göre küçük, düşük profilli, üretimi ve entegrasyonu kolay ve uygun maliyetli olma avantajlarına sahip olup ikili ve üçlü çalışma frekanslarını desteklemektedir.

Bu tez çalışmasının temel amacı, 5G haberleşme sistemlerinde kullanılabilecek çift çalışma bantlı MIMO mikroşerit antenler tasarlamaktır. Bunun için ilk önce dört elemanlı, 1.55 mm yükseklikli, FR-4 alt tabakalı bir mikroşerit anten tasarlanmıştır. İlk tasarım 4 × 4 MIMO şeklinde olup çalışma frekansları 26 GHz ve 38 GHz'dir. Daha sonra ABD standardına uygun ve 28 ve 38 GHz'de çalışan bir anten tasarımı yapılmıştır. Bu çalışmada antenin güçlü ve zayıf yönlerini belirlemek ve optimize etmek için CST yazılımı kullanılmıştır.

Tasarlanan ilk anten 23 - 28.5 GHz ve 35 - 39.5 GHz frekans aralıklarında çalışmaktadır. Antenin 26 GHz'de kazancı 9.86 dBi olup bu frekanstaki verimi %60'ın üzerindedir. 38 GHz frekansında ise kazancı 6.71 dBi, verimi ise %50'nin üzerindedir.

Tasarlanan ikinci anten 26 - 31 GHz ve 34.5 - 40 GHz frekans aralığında çalışmakta olup, 28 GHz'deki verimi %70'in üzerinde, kazancı 10.6 dBi'dır. 38 GHz'de frekansında ise kazancı 6.65 dBi iken verimi %50'nin üzerindedir.

Simülasyon sonuçlarına göre tasarlanan her iki anten için de ortalama izolasyon birinci bantta -20 dB ve ikinci bantta -30 dB'dir. Ayrıca DG yaklaşık 10 dB, ECC 1 × 10^{-6}'den daha düşüktür. Bu değerler literatürdeki benzer anten tasarımları ile karşılaştırıldığında oldukça iyi düzeydedir.

Anahtar Sözcükler: 5G, mm-dalga, MIMO, Mikroşerit anten, CST

ABSTRACT

MIMO ANTENNA DESIGN FOR 5G MILLIMETER-WAVE
COMMUNICATION SYSTEMS

Nermin K.A. HAMDAN
Ondokuz Mayıs University
Institute of Graduate Studies
Department of Electrical and Electronics Engineering
Master, January/2023
Supervisor: Assoc. Prof. Dr. Çetin KURNAZ

One of the most sought-after research topics in telecommunication is the 5G antenna design which needs continuous improvement. The channel capacity of the 5G system is increased by using the microstrip MIMO antenna. MIMO is an antenna technology that utilizes several antennas to provide performance improvements. Whereas, microstrip antenna has the advantages of being small, low-profile, easy to manufacture and integrate, and affordable over other types of antennas. Also, one patch can reinforce dual and triple resonant frequencies.

The main objective of this thesis is to design a dual-band MIMO microstrip antenna for serving the 5G communication system. Initially, the proposed four-element structure contained a slotted microstrip antenna based on an FR-4 substrate with a height of 1.55 mm. The first design was a 4 × 4 MIMO operating at 26 and 38 GHz. Then, numerous procedures were applied to the first design to comply with the U.S. standard, which operates at 28 and 38 GHz. These were continuously generated with the CST software simulations to identify the antenna's strengths and weaknesses and optimize them accordingly.

The first design of the proposed antenna operates from 23 to 28.5 GHz and from 35 to 39.5 GHz. At 26 GHz, it features a gain of 9.86 dBi with a radiation efficiency of more than 60%. While at 38 GHz, it features a gain of 6.71 dBi with a radiation efficiency of more than 50%.

The second design operates from 26 to 31 GHz and from 34.5 to 40 GHz. A high gain of 10.6 dBi with an efficiency of more than 70% was featured at 28 GHz. While at 38 GHz, it features a high gain of 6.65 dBi and an efficiency of 50%.

For both designs, we figured out that the average isolation is -20 dB and -30 dB at the first and second bands, respectively, according to simulation results. As well, the DG is nearly 10 dB, and the ECC is less than 1×10^{-6}, providing excellent performance compared to previous antenna designs.

Keywords: 5G, mm-wave, MIMO, Microstrip antenna, CST

ACKNOWLEDGEMENT

In the first place, I would like to express my great gratefulness to Allah, who has blessed me with the will and ambition to carry out this thesis.

Unsurprisingly, my mother was the most supportive person throughout this journey. She has been more than just a mother. She helped, supported, and traveled all the way from Palestine to Turkey to be by my side. Great, thanks go to her endless love.

Thanks to my father and two brothers for believing in me and my abilities to achieve my dreams.

Of course, my sincere appreciation goes to my great supervisor: Assoc. Prof. Dr. Çetin Kurnaz. He has always been supplying me with the required knowledge and advice to get the best out of this work.

Last but not least, thanks to my close friend in Palestine and my good friends in Turkey.

Nermin K.A. HAMDAN

CONTENTS

ACCEPTANCE AND APPROVAL OF THE THESIS i
DECLARATION OF COMPLIANCE WITH SCIENTIFIC ETHIC............................ ii
DECLARATION OF THE THESIS STUDY ORIGINALITY REPORT ii
ÖZET iii
ABSTRACT iv
ACKNOWLEDGEMENT v
CONTENTS vi
SYMBOLS AND ABBREVIATIONS vii
FIGURES LEGENDS viii
TABLES LEGENDS ix
1. INTRODUCTION 1
1.1. Literature Review 2
1.2.Thesis Scope and Objective 7
2. GENERAL INFORMATION 8
2.1. Introduction to Antenna 8
2.2. Antenna Types 8
2.2.1. Wire Antennas 8
2.2.2. Aperture Antennas 9
2.2.3. Reflector Antennas 9
2.2.4. Lens Antenna 10
2.2.5. Microstrip Antennas 10
2.2.5.1. Feeding Methods 11
2.2.5.1.1. The Contacting Feeding Methods 11
2.2.5.1.2. The Non-Contacting Feeding Methods 12
2.3. Antenna Parameters 12
2.3.1. Radiation Pattern 12
2.3.2. Directivity 13
2.3.3. Gain 13
2.3.4. Antenna Efficiency 14
2.3.5. Resonant Frequency 14
2.3.6. Input Impedance 14
2.3.7. Bandwidth 15
2.3.8. Polarization 15
2.3.9. VSWR 16
2.3.10. Return Loss 16
2.4. The Fifth Generation 5G 17
2.4.1. The Frequency Bands of 5G 18
2.5. Millimeter-Wave 19
2.6. Standards of 5G mm-wave Frequency Bands 21
2.7. MIMO Technology 22
2.7.1. Performance Parameters of MIMO 23
2.7.1.1. Envelope Correlation Coefficient 23
2.7.1.2. Diversity Gain 24
3. MATERIALS AND METHODS 25
3.1. Software Requirements 25
3.2. Hardware Requirements 25
3.3. Antenna Design 26
4. RESULTS AND DISCUSSION 31
4.1. The results of the single antenna 31

4.2. The results of the first designed antenna....32
4.3. The results of the second designed antenna....42
5. DISCUSSION....52
5.1. Antenna Comparison....52
6. CONCLUSION....54
6.1. Future work....55
REFERENCES....56
CURRICULUM VITAE....60

SYMBOLS AND ABBREVIATIONS

CST	: Computer Simulation Technology
DG	: Diversity Gain
DGS	: Defective Ground Structure
ECC	: Envelope Correlation Coefficient
ITU	: International Telecommunications Union
MIMO	: Multiple-Input Multiple-Output
mm-Wave	: Millimiter-wave
MPA	: Microstrip Patch Antenna
SMA	: Standard male connector
VSWR	: Voltage Standing Wave Ratio
1G	: First Generation
2G	: Second Generation
3G	: Third Generation
3GPP	: Third Generation Partnership Project
4G	: Fourth Generation
5G	: Fifth Generation

FIGURES LEGENDS

Figure 2.1. Forms of wire antennas 9
Figure 2.2. Aperture antenna forms 9
Figure 2.3. Reflector antenna forms 10
Figure 2.4. Microstrip patch antenna 11
Figure 2.5. Patches in different forms 11
Figure 2.6. Types of radiation pattern 13
Figure 2.7. Bandwidth Form 15
Figure 2.8. Polarization type 15
Figure 2.9. Resonance frequency at 28 GHz return loss 16
Figure 2.10. Mobile wireless evolution 18
Figure 2.11. 5G frequency bands. 18
Figure 2.12. Spectrum coverage of 1G,2G,3G,4G, and 5G 19
Figure 2.13. Features of different frequency bands 19
Figure 2.14. Millimeter-wave frequencies 20
Figure 2.15. 5G mm-wave frequency bands 22
Figure 2.16. Atmospheric Attenuation across mm-wave Band 23
Figure 2.17. MIMO system 23
Figure 3.1. CST program 25
Figure 3.2. Standard connector SMA 26
Figure 3.3. a) Microstrip antenna, b) Top view of the antenna 27
Figure 3.4. A step-by-step for designing the single antenna a) phase 1, b) phase 2, c) phase 3, d) phase 4, e) Ground is the same for b and c phase 28
Figure 3.5. a) front, b) back side of the suggested first design 29
Figure 3.6. a) front, b) back side of the suggested second design 30
Figure 4.1. A single antenna design's return loss for each stage 31
Figure 4.2. Each port's reflection coefficients of the first designed MIMO antenna 32
Figure 4.3. Ports' isolation between each patch antenna of the first MIMO 33
Figure 4.4. The 3D-dimensional radiation pattern at 26 GHz of a) port 1, b) port 2, c) port 3, d) port 4 34
Figure 4.5. The polar radiation pattern at 26 GHz of a) port 1, b) port 2, c) port 3, d) port 4 35
Figure 4.6. The 3D-dimensional radiation pattern at 38 GHz of a) port 1, b) port 2, c) port 3, d) port 4 36
Figure 4.7. The polar radiation pattern at 38 GHz of a) port 1 b) port 2, c) port 3, d) port 4 37
Figure 4.8. Antenna efficiency of each port of the first MIMO antenna 38
Figure 4.9. The ECC performance for the first designed MIMO antenna 38

Figure 4.10. The DG performance for the first designed MIMO antenna 39
Figure 4.11. The surface current of a) the first port, b) the second port, c) the third port, d) the fourth port of the first design at 26 GHz.. 40
Figure 4.12. The surface current of a) the first port, b) the second port, c) the third port, d) the fourth port of the first design at 38 GHz... 41
Figure 4.13. Each port's reflection coefficients of the final designed MIMO antenna 42
Figure 4.14. Ports' isolation between each patch antenna of the final MIMO 43
Figure 4.15. The 3D-dimensional radiation pattern at 28 GHz of a) the first port, b) the second port, c) the third port, d) the fourth port 44
Figure 4.16. The polar radiation pattern at 28 GHz of a) the first port, b) the second port, c) the third port, d) the fourth port 45
Figure 4.17. The 3D-dimensional radiation pattern at 38 GHz of a) the first port, b) the second port, c) the third port, d) the fourth port 46
Figure 4.18. The polar radiation pattern at 38 GHz of a) the first port, b) the second port, c) the third port, d) the fourth port 47
Figure 4.19. Antenna efficiency of each port of the final MIMO antenna 48
Figure 4.20. The performance of ECC for the second design 48
Figure 4.21. The performance of DG for the second design 49
Figure 4.22. The surface current of a) the first port, b) the second port, c) the third port, d) the fourth port of the second design at 28 GHz 50
Figure 4.23. The surface current of a) the first port, b) the second port, c) the third port, d) the fourth port of the second design at 38 GHz 51
Figure 6.1. a) front, b) back side of the fabricated single antenna 55
Figure 6.2. a) front, b) back side of the fabricated first MIMO antenna 55

TABLES LEGENDS

Table 3.1. The material’s characteristics 26
Table 3.2. A single antenna’s dimension 29
Table 4.1. Port’s ECC value between each patch antenna of the second MIMO 39
Table 4.2. Port’s ECC value between each patch antenna of the second MIMO 49
Table 5.1. Comparing the proposed antenna to other papers 52

1. INTRODUCTION

Wireless communication technology has changed the way we communicate and socialize in a remarkable way since its inception. It helped us to transmit data over a distance without any cables. Also, the ability to communicate with people on move has developed arrestingly. The several generations of wireless communication over time were one of the main reasons to lead to a revolution in mobile communication. Because of the incredibly high number of connected devices and the lack of bandwidth, wireless communication has been updated to fifth-generation (5G). 5G seeks to improve mobile network data rates, scalability, connectivity, and energy efficiency.

In the research fields of telecommunications, the 5G antenna design is one of the most sought-after topics. As technology develops, user demands are also increasing. In order to cope with this demand, millimeter-wave (mm-wave) frequencies for unused spectrum are used in favor of the 5G. According to the International Telecommunications Union (ITU), the bands of 27.5-29.5 GHz, 33.4-36.5 GHz, 37-40 GHz, 47-50.2 GHz, and 59.3-71.1 GHz are defined as the 5G mm-wave (Khattak, 2019). It is expected that 5G mobile communications will operate primarily in the 26, 28, and 38 GHz because the absorption of electromagnetic waves in these bands in the atmosphere is low.

5G systems require higher capacity and large bandwidth. Microstrip patch antenna (MPA) has many outstanding features, like lightweight and small size, which make it popular in wireless communications (Zakariyya, 2016). However, the Multiple-Input Multiple-Output (MIMO) antennas have always been an essential factor in wireless systems. Aside from this, it offers multipath propagation with higher data rates and greater capacity; which are considered some of the key characteristics of the 5G (Rahman, 2019). This thesis's main objective is designing two structures of 4 × 4 MIMO antenna operating on different mm-wave bands in a dual-band mode. Initially, to accomplish this objective, a rectangular microstrip antenna, as part of the required four-element design, will be proposed. As well, CST Microwave Studio will be utilized to simulate antenna characteristics.

1.1. Literature Review

The aim of this chapter is to serve as a source of comparison by analyzing the previous references and deriving a result that is better for the antenna that will be designed. The literature has demonstrated several antenna solutions for 5G mm-wave bands.

In (Tu et al, 2017), the authors have proposed a four-element antenna that resonates at two different bands for 5G applications. Rogers 5880 is the basis for the design with dimensions of 19.25 × 26 × 0.79 mm. The offered MIMO antenna provides dual-band operation from 27.5 to 30 GHz and 37 to 39 GHz. In the first band, it has a return loss of nearly -35 dB and a gain of 7 dBi, whereas, in the second band, it has a -30 dB return loss and 5 dBi gain. By using novel round patch cells with electromagnetic bandgap, for all operating bands, it achieves low mutual coupling. And for both bands, the envelope correlation coefficient (ECC) is below 0.004.

In (El Mashade and Hegazy, 2018), the authors have offered a 4x1 array antenna that oscillates at 28 GHz. This antenna was first designed as a signal microstrip patch antenna, then it was designed as two elements, and then it was designed as four elements. Furthermore, it operated from 27 to 28.3 GHz. The design was developed on an FR-4 measuring 31.677 × 7.07 × 0.1 mm in size. This antenna has almost a -21.44 dB return loss at 28 GHz. Moreover, it also provides a gain and efficiency of more than 8.5 dBi and 70%, respectively.

In (Rahayu et al, 2018), the authors have reported a four-element MIMO antenna feeding by a microstrip line, with an overall Duroid 5880 substrate size of 25 × 25 × 1.575 mm. It has operated from 27.10 to 28.88 GHz. The simulated results indicate 8 dBi gain, 70% efficiency, and a return loss of about -32 dB. Besides that, the author provided no analysis of MIMO antenna performance.

In (Hasan et al, 2019), the authors have demonstrated a 2 × 2 MIMO antenna at mm-wave bands. The design is based on a Rogers 5880 with a dimension of 14 x 26 x 0.38 mm. The proposed antenna offers a dual-band operation from 26.65 to 29.2 GHz and 37 to 39.05 GHz. It also provides nearly -35 dB return loss on both bands and isolation of below -20 dB. The ECC is below 0.001 in both bands. In addition, the antenna has a gain of nearly 1.27 dBi at 28 GHz, while at 38 GHz it has nearly 1.83

dBi and shows an omnidirectional pattern and an efficiency of 75%.

In (Marzouk et al, 2019), the authors have demonstrated a printed MIMO antenna. The paper suggests three designs, the first design is a rectangular microstrip antenna and one feed, the second is a symmetrical rectangular microstrip antenna with two elements, and the last one is a symmetrical MIMO antenna with four elements and slotted rectangular patches. The designs were developed on a Rogers RO4003 measuring 55 × 110 × 0.508 mm in size. It operated from 27-28.5 GHz and 37-39 GHz. It has nearly -21.57 dB return loss at 28 GHz, while at 38 GHz it has -24.59 dB, and the antenna has an isolation port of -26 dB. Furthermore, it is characterized by low mutual coupling and a desirable ECC and has a gain of nearly 7.95 dBi at 28GHz, while at 38 GHz it has nearly 8 dBi.

In (Shuhrawardy et al, 2019), the researchers have presented a 4 × 4 compact wideband MIMO antenna for mm-wave frequencies. The design is based on a Rogers 5880 with a dimension of 30 × 25 × 0.8 mm. Each element consists of a patch with a slot-shaped of an inverted F, and a slotted ground plane. Based on -10 dB, as a return loss, It operates from 26.6 to 39 GHz covering almost three bands. Moreover, it has a 5.28 dBi maximum gain and isolation below -20 dB. In addition, the antenna has an ECC of less than 0.002.

In (Sehrai et al, 2020), the authors have suggested a 4 × 4 MIMO antenna that performs at mm-wave for 5G. The radiating element of the design consists of four different arcs. The design is based on a Rogers 5880 with a dimension of 80 x 80 x 1.57 mm. Based on the -10 dB criterion, the suggested antenna operates in the 23 to 40 GHz range. It has more than -20 dB isolation, 10 dBi gain, and total radiation efficiency of above 70%. It also observed that the ECC is less than 0.0014.

In (Khalid et al, 2020), the researchers have presented a four-port MIMO structure with a 30 × 35 mm substrate size. It uses Rogers R04350B as a substrate with a height of 0.76 mm. It operates from 25.5 to 29.6 GHz. Furthermore, the gain achieved in the operating band is 7 dBi and efficiency is over 70%. As well, the ECC is less than 0.01 and the isolation is more than -10 dB.

In (El Hadri et al, 2020), the authors have presented an antenna with a compact 2 × 2 MIMO design that provides high isolation and low ECC at 28 GHz. The design is based on an FR-4 with a dimension of 12.8 × 26 × 1.6 mm. It also covers a range from 27.5- 28.35 GHz.The antenna has a return loss of nearly -35 dB and port isolation of more than -30 dB. Further, the presented MIMO antenna achieves a good ECC below .0000115 and a diversity gain (DG) of 10 dB since it uses a spatial diversity technique. Also, the gain and efficiency of the offered design are 7 dBi and more than 60 %, respectively.

In (Desai et al, 2020), the researchers have presented a 4 × 4 MIMO antenna that is compact, transparent, and has a full ground with a microstrip feed line. It is based on a Rogers 5880 with a dimension of 24 × 20 × 1.85 mm. The proposed MIMO antenna offers a dual-band operated from 24.10 to 27.18 GHz with 3.08 GHz of bandwidth and 33 GHz to 40 GHz with 7 GHz of bandwidth. The antenna at the resonant frequencies has almost a -25 dB return loss and good isolation of more than -16 dB. Additionally, it shows 3 dBi gain and 75% efficiency at the resonance bands. And at both bands, the antenna has an ECC below 0.1 and a DG above 9.5.

In (Hakim et al, 2020), the authors have displayed a 2 × 2 MIMO antenna that resonates at two different bands for 5G applications. In order to achieve dual-band and wide bandwidth, a stub slot and a defective ground structure (DGS) have been employed. The design is based on an air substrate with a dimension of 21.96 × 16.71 × 0.5 mm. The suggested design performs from 25 to 29 GHz and 35 to 45 GHz. Moreover, It has nearly 8.35 dBi gain at 28GHz, while at 38 GHz it has nearly 6.48 dBi. The designed MIMO provides low isolation below -20 dB.

In (Rahman et al, 2020), the authors have offered a novel MIMO antenna inspired by nature that is suitable to perform at 28 GHz. The design is modeled on a Rogers 5880 with dimensions of 30 × 30 × 0.787 mm. At the resonant frequency, it has almost a -32 dB return loss. The proposed system's gain and efficiency are 6 dBi and less than 70%, respectively. Furthermore, performance parameters in MIMO, which include ECC and DG are below 0.15 and 10, respectively.

In (Amrutha et al, 2021), the authors have reported a compact ultra-wideband antenna with a high-isolation 2 x 2 MIMO antenna. The presented design consists of two fork-shaped antenna, and the two patches are arranged perpendicular to each other. It is also based on a Rogers-5880 substrate with a dimension of 11 × 7.5 × 0.762 mm. The designed antenna covers a range from 34 to 39 GHz. It also has nearly -25 dB return loss and port isolation of less than -22 dB. Regarding performance parameters in MIMO, which include ECC and DG show acceptable results which, assure the prototype's excellent MIMO performance.

In (Sehrai et al, 2021), the authors have designed a compact 4 × 4 MIMO antenna at mm-wave bands for 5G. It is built on a Rogers 5880 with a dimension of 23.7 × 8.8 × 0.5 mm. The proposed MIMO antenna provides wideband operation from 36.83 to 40 GHz. It has gain and efficiency values of 6.5 dBi and less than 80% and good isolation below -30 dB at the resonant frequencies. Concerning performance parameters in MIMO, which include ECC and DG show acceptable results, confirming the excellent MIMO performance of the prototype.

In (Saleem et al, 2021), the authors have proposed a 4 × 4 MIMO compact slot-based antenna for a 5G mm-wave. It is built on a Rogers 5880 with a dimension of 14 × 14 × 0.79 mm. The proposed MO antenna presents a dual-band operated from 27.5 to 30.25 GHz and 37 to 40 GHz. In the first band, the design has less than -20 dB return loss, while in the second band it has less than a -25 dB. Furthermore, it shows a gain of about 7.09 dBi and 3.43 dBi in the first and second bands, respectively. Also, good isolation of less than -24 dB at 28 GHz and -17 dB and 38 GHz. And at the resonant frequencies, the ECC is below 0.014.

In (Ghosh and Swati, 2021), the authors have demonstrated a 2 × 2 MIMO antenna that oscillates at 28 GHz. Each of the antenna’s radiating elements is perpendicular to the other and each consists of a rectangular slotted patch. A Rogers-5880 substrate with a dimension of 40 × 18.607 × 0.508 mm is used for the antenna design. The proposed antenna operated from 27.8 to 28.8 GHz and it has a return loss and port isolations of almost -22 dB and over -25 dB, respectively. The gain is also nearly above 10 dBi. Regarding performance parameters in MIMO, which include ECC and DG show acceptable results which, assure the prototype's excellent MIMO performance.

In (Awan et al, 2021), the authors have proposed a compact printed wideband antenna for millimeter wave bands based on DGS. It was developed on a Rogers RO4003 with a 15 × 15 × 0.203 mm dimension. The offered design operates from 27 to 30 GHz. In addition, it offers a return loss of nearly -22 dB. It also has a gain of nearly 5.69 dBi and an efficiency of more than 75% in the operating bandwidth.

In (Raheel et al, 2021), the researchers have presented a 4 × 4 MIMO antenna performing at 28 and 38 GHz bands for 5G communications. It is based on a Rogers-

5880 substrate with 20 × 24 × 0.508 mm dimensions. Three parts make up each radiating element: a slot-shaped of E, a slot-shaped of H, and a transmission line. The antenna has -18 dB return loss at 28 GHz and -20 dB at 38 GHz, and again of 7.1 dBi at 28 GHz and 7.9 dBi at 38 GHz, with efficiencies of less than 85%, and an ECC below 0.001.

In (Kamal et al, 2021), the authors have designed a 4 × 4 MIMO antenna for mm-wave. Each patch of this antenna is circular ring-shaped, and it resonated at 28 GHz with 1.5 GHz bandwidth. It has a return loss of -35 dB and port isolation of -18 dB. As a substrate, Rogers-5880 is used with dimensions of 30 × 30 × 0.787 mm. The design achieves a maximum gain of 5.5 dBi. The ECC analysis also revealed that it is less than 0.16.

In (Sabek et al, 2021), a monopole antenna with triangle stubs was proposed. As a substrate, Rogers RO4003 is used with dimensions of 12 × 12 × 0.237 mm. The proposed antenna offers a dual-band operated from 25.9 to 30.4 GHz and 36.4 to 40.2 GHz. The antenna offers less than -20 dB return loss at both bands. In addition, the antenna has a gain of nearly 4.5 dBi and an efficiency of more than 80% at the resonant frequencies.

In (Desai and Neelgar, 2021), the authors have proposed a 4 × 4 rectangular patch MIMO antenna at the mm-wave frequency and fed with a microstrip line. The MIMO antenna aims to resonate at 26 GHz, which operates from 24.2 to 26.59 GHz and has a port isolation of more than -23 dB. The antenna is modeled on a Rogers 5880 with dimensions of 15 x15 x 0.5 mm. The proposed antenna's gain and efficiency are 5.38 dBi and less than 80%, respectively. Furthermore, the ECC is below 0.005.

In (El Hadri et al, 2022), the authors have presented an antenna with a compact, wide 2 x 2 MIMO design that provides high isolation and low ECC at 38 GHz. As a substrate, FR-4 is used with dimensions of 12.8 × 26 × 1.6 mm. As well, the space between the two patches is 1 mm. Further, the designed antenna covers a band range from 34 to 45 GHz. It also has a return loss of nearly -33 dB, port isolation of more than -25 dB, a gain of 7 dBi, and an efficiency of more than 70%. Further, the presented MIMO antenna achieves a good ECC of more than 0.0002 and the DG is about 10 dB by using the spatial diversity technique.

In (Chaudhary and Kansal, 2022), the authors have proposed a dual-band 2 × 2

MIMO antenna working in 5G mm-wave. The antenna is designed with two MIMO antennas placed antiparallel to each other; each antenna consists of two mirror-image C-shaped strips centered on an off-centered fed patch. Also, the design is based on a Rogers 5880 with a dimension of 10 × 17 × 0.324 mm. The proposed MIMO antenna offers a dual-band operated from 27.9 to 28.45 GHz and 37.5 to 38.5 GHz. Furthermore, it shows a gain of 7.46 dBi at 28 GHz and 8.56 dBi at 38 GHz. Regarding performance parameters in MIMO, which include ECC and DG show acceptable results which, assure the prototype's excellent MIMO performance.

In (Manirathnam et al, 2022), the authors have exhibited a compact 2 × 2 MIMO antenna that oscillates at 28 GHz. An antenna's radiating elements are perpendicularly arranged. The design is based on a Rogers 5880 with a dimension of 22 × 12 × 0.8 mm. It also operated from 27.25 to 28.73 GHz. At the resonant frequency, the antenna has return loss and port isolations of nearly -38 dB and over -25 dB, respectively. In addition, the gain is nearly 6.82 dBi. As far as performance parameters in MIMO are concerned, the design's envelope correlation coefficients and diversity gain have shown acceptable results.

1.2. Thesis Scope and Objective

This thesis aims to design two structures of 4 × 4 MIMO antenna. It was suggested that the first design will operate at 26 and 38 GHz bands while the second design at 28 and 38 GHz bands. Both designs’ sizes are supposed to be compact and simultaneously provide wide bandwidth and good gain. The MIMO antenna is made of four microstrip patches, so it helps in increasing the capacity of the wireless communication channel when a single antenna element is insufficient. This problem can be solved by using MIMO. Moreover, MIMO has become an indispensable aspect that is constantly used by high-end 5G telecommunication systems. Due to this, the proposed antenna will be powered by MIMO in order to produce better results.

2. GENERAL INFORMATION

In this chapter, the fundamentals of antennas and the needed measures to evaluate the antenna's usability will be presented. In addition, a better understanding of the antenna's way of design will be demonstrated by discussing the 5G mm-wave frequencies and MIMO performance parameters.

2.1. Introduction to Antenna

The antenna is a significant component in any mobile communication system. It is a device that can transmit and receive electromagnetic energy (Ojaroudiparchin, and Pedersen, 2015). Basically, on the transmitting side, it converts the received electrical pulses into electromagnetic signals that propagate to the receiving device, while on the receiving side, it intercepts the electromagnetic pulses and converts them into electrical pulses that are then transmitted to the antenna (Harrington, 1960). In other words, the antenna acts as a transit point between the medium of the transmission line and the boundless medium in which the electromagnetic energy propagates. An antenna can come in all sizes. Its size relays mainly on the application and the frequency band for which it is used. The antenna's size is proportional to the length of the wave it directly transmits or receives. Further, the antenna's size decreases as the frequency range increases. Therefore, cell phones operate at high frequencies since they are small devices (Khan, 2017).

2.2. Antenna Types

The size along with the design of the antenna is well-known for giving each antenna its unique characteristics and making it usable in specific applications. Accordingly, antennas are divided into multiple types with different fields of utilization. The most prominent ones are discussed below.

2.2.1. Wire Antennas

These are considered to be the most versatile, and cheapest antennas, as well as are widely known to people since they can be found almost anywhere, on cars, buildings, ships, and airplanes. Wire antenna begins acting as an antenna, picking up and radiating signals as soon as the wire leaves the antenna tower. Further, in most cases, they can adapt to many applications. Figure 2.1 shows three types of wire antennas: dipoles, loops, and helices (Balanis, 2012).

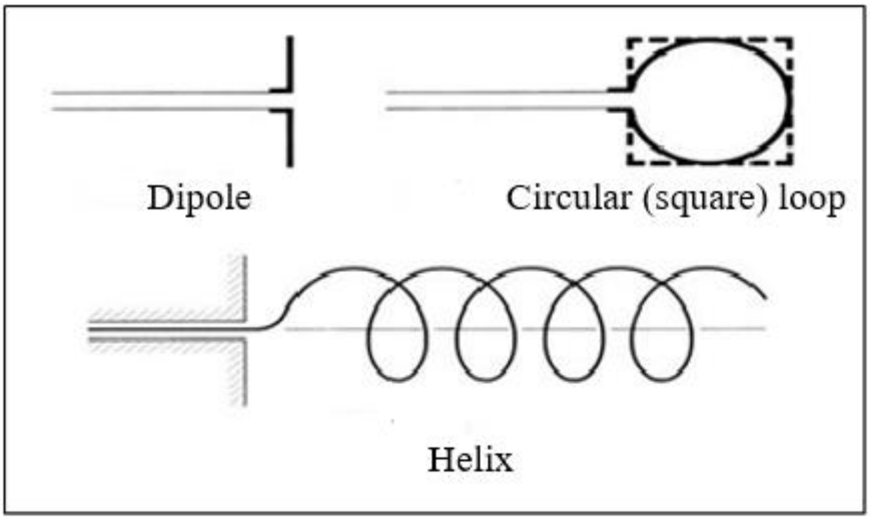

Figure 2.1. Forms of wire antennas (Balanis, 2012)

2.2.2. Aperture Antennas

These are considered to be a type of directional antenna which is most commonly used at microwave frequencies. The antenna aperture is an area around a device that produces power when an electromagnetic field is applied. It has a wide range of geometrical configurations, such as waveguides and horns whose aperture is square, rectangular, circular, elliptical, or any combination thereof as shown in Figure 2.2. Furthermore, the use of these antennas in aircraft and spacecraft is extensive.

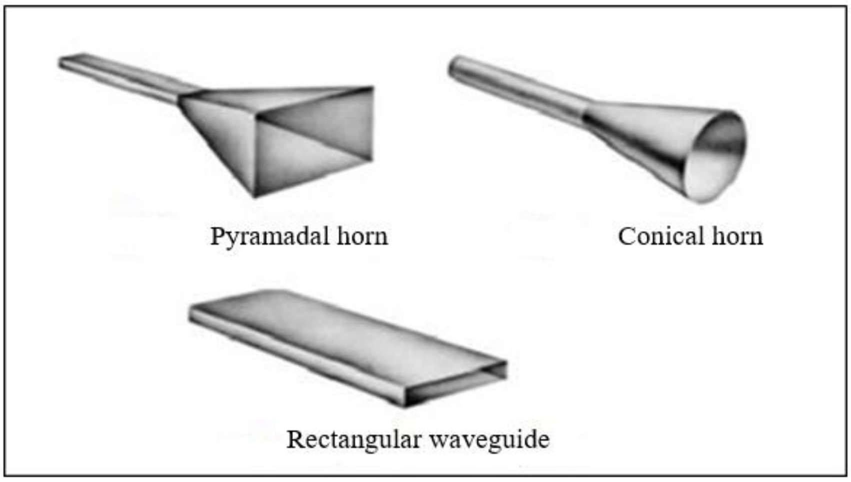

Figure 2.2. Aperture antenna forms (Balanis, 2012)

2.2.3. Reflector Antennas

A reflector antenna is one the most commonly used on spacecraft since it is lightweight and simple structure. Reflector antennas are composed of a reflecting surface and a feeding system. Also, the excellent radiation characteristics, versatility, and manufacturing readiness make this material ideal for radars, deep-space telemetry, radio astronomy, and satellite communications. As illustrated in Figure 2.3, a parabolic reflector is one of the most common antenna forms for such applications.

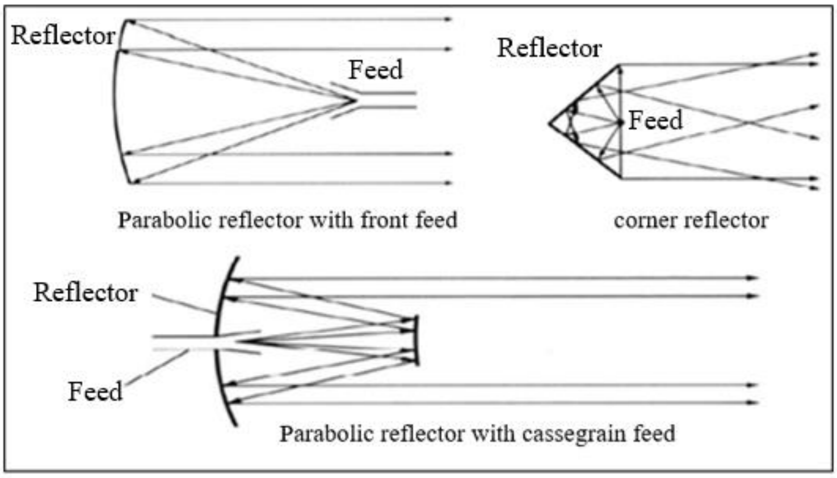

Figure 2.3. Reflector antenna forms (Balanis, 2012)

2.2.4. Lens Antenna

These are microwave antennas that use shaped, microwave-transparent materials to bend and focus radio waves, much like optical lenses bend and focus light. A lens antenna is made of glass and follows the converging and diverging characteristics of a lens. A lens antenna can be either a dielectric or metal plate lens antenna. In lens antennas, the feed antennas in the design do not block the aperture, which is one of their main advantages. However, a lens antenna has the disadvantage of being more expensive than a reflector antenna for the same gain/bandwidth.

2.2.5. Microstrip Antenna

The microstrip antenna has a crucial role in wireless communication technology today and is one of the most popular types of printed antennas. Further, it is common to be called a patch antenna (Joshi and Gond, 2017). It is made of a very thin metal strip positioned on a ground plane with a dielectric material in between as shown in Figure 2.4. Antennas of microstrip are used in many prominent applications including airships, space technology, and satellites where size, design, weight, and structure are all significant since microstrip antennas are a standout among other contenders to meet these requirements.

A microstrip patch antenna has the advantages of being small, low-profile, easy to manufacture and integrate, and affordable over other types of antennas. Moreover, one patch can reinforce dual and triple resonant frequencies, in addition to linear and circular polarization (Ang and Chung, 2007).

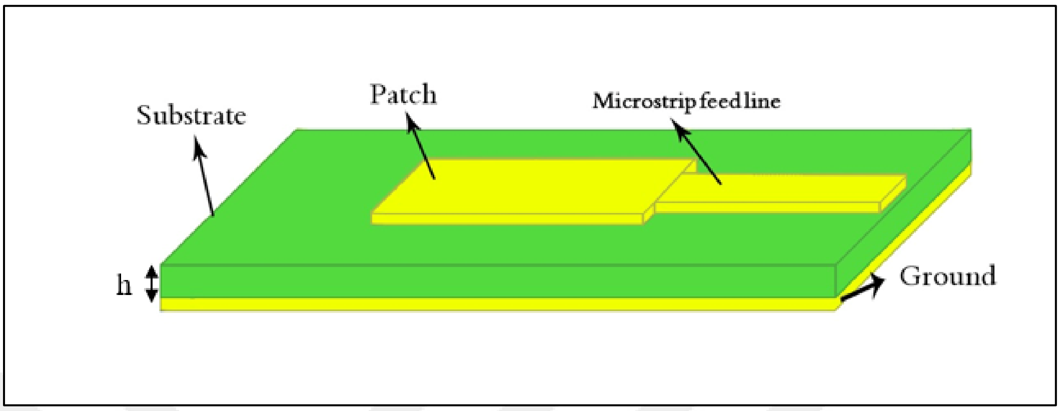

Figure 2.4. Microstrip patch antenna

Furthermore, the patch is typically square, circular, or rectangular as Figure 2.5 illustrate.

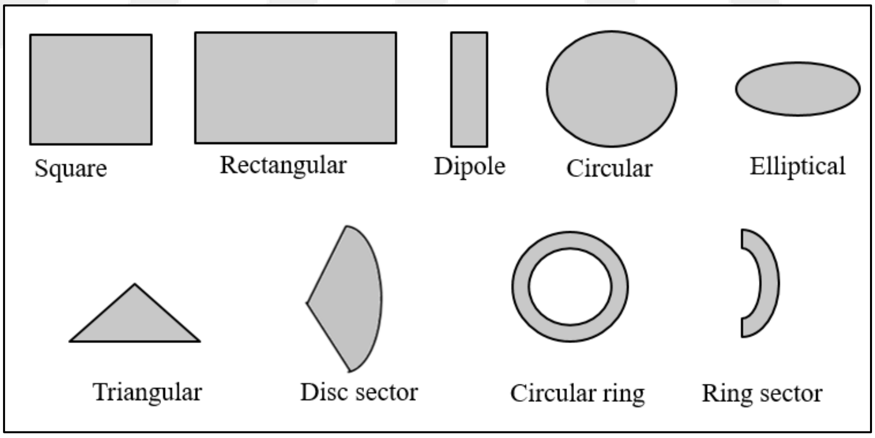

Figure 2.5. Patches in different forms (Balanis, 2012)

2.2.5.1. Feeding Methods

Various methods can be used to feed a microstrip antenna. There are two main categories of these methods: contacting and non-contacting.

2.2.5.1.1. The Contacting Feeding Methods

This method of feeding the radiating element is directly connected to the feed line. Like coaxial feeding, this method uses a coaxial cable with two conductors the inner one connects to the patch, whereas the outer connects to the ground through a hole drilled in the substrate. Similar to microstrip inset feed lines, this design integrates the feed line and radiating patch into a single layer.

2.2.5.1.2. The Non- Contacting Feeding Methods

This type of feeding relies on electromagnetic feeding, in which the feed line is not directly connected to the radiating element. As with aperture coupling feed, this type has a ground with an aperture that lies between two substrates. Also, on the top side, the patch lies whereas the transmission line lies on the bottom. Similar to proximity coupling feed, a transmission line is sandwiched between two substrates and it has an upper radiation patch and a lower ground patch.

2.3. Antenna Parameters

Several parameters have a significant influence on antenna performance. Therefore, the following parameters must be analyzed when designing and measuring antennas. The basic antenna parameters are listed below (Balanis, 2005).

2.3.1. Radiation Pattern

It is one of the significant parameters of any antenna. It is a graphical representation of the antenna's radiation properties as a function of space as it describes how strongly an antenna radiates in any given way. A radiation pattern is displayed in the far field as well as in the 2D and/or 3D fields. Radiation patterns are in general presented on a linear, logarithmic scale, or in decibels (Balanis, 2005).

Each antenna radiates differently, but all can be classified into one of three main types as shown in Figure 2.6.

The isotropic antennas radiate their power uniformly in all directions like a sphere, which is possible only in theory. Therefore, the isotropic pattern is usually a useful reference point to explain how practical antennas radiate in a particular direction.

While the omnidirectional antenna radiates uniformly in all directions of a plane. In contrast, the directional antenna focuses its radiation in a certain direction.

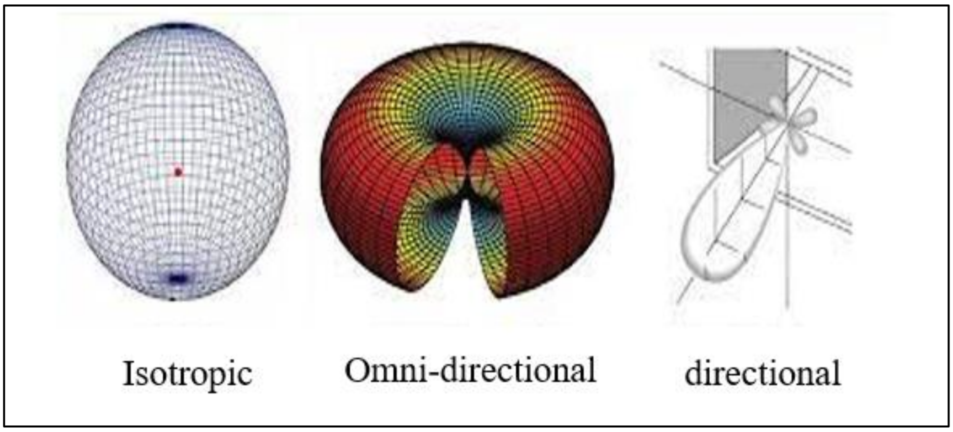

Figure 2.6. Types of the radiation pattern (Aironet, 2007)

2.3.2. Directivity

One of the basic antenna parameters is directivity. It is a scale that measures the directivity of an antenna's radiation pattern. Also, the antenna can direct power in a particular direction in a sending or receiving situation. Additionally, directivity is measured in dBi, which stands for isotropic. Equation (2.1) gives the mathematical formula for directivity (Balanis, 2005).

$$D = \frac{U}{U_o} = \frac{4\pi U}{P_{rad}} \tag{2.1}$$

As (U) represent radiation intensity (RI) whereas (U_o) represent (RI) of the isotropic source and (P_{rad}) is the total radiated power.

2.3.3. Gain

Gain is another useful parameter for evaluating antenna performance. In contrast to directivity, which depends only on the antenna pattern, gain takes into account both the antenna's directivity and efficiency. The gain, therefore, is a measure of how efficiently an antenna turns its input power into radiated power in a given direction as compared to an isotropic source. Equation (2.2) gives the mathematical formula for the gain (Küpeli et al, 2017).

$$G = 4\pi \frac{U(\theta,\emptyset)}{P_{in}} \tag{2.2}$$

As (G) is the gain, (U) is the radiation intensity in the direction of $(\theta, \emptyset)$, and (P_{in}) is the input power.

$$P_{in} = \frac{P_{rad}}{e_{cd}} \tag{2.3}$$

$$e_{cd} = e_c e_d \tag{2.4}$$

Where (P_{rad}) is the total radiated power, (e_{cd}) is the antenna efficiency,(e_c) is the conduction efficiency, and (e_d) is the dielectric efficiency.

$$G(\theta,\emptyset) = e_{cd}\left[4\pi\frac{U(\theta,\emptyset)}{P_{rad}}\right] \tag{2.5}$$

As a result, we get the following equation (2.6) when we substitute equation (2.1) into equation (2.5).

$$G(\theta,\emptyset) = e_{cd}D(\theta,\emptyset) \tag{2.6}$$

As $G(\theta,\emptyset)$ is the gain and $D(\theta,\emptyset)$ is the directivity, and both are in the direction of $(\theta,\emptyset)$.

2.3.4. Antenna Efficiency

It is the proportion between the power it radiates and the total input power it receives. As with any other electrical device, losses occur between the input and output of the antenna. Therefore, only a theoretical antenna can achieve 100% efficiency. Furthermore, compared to low-efficiency antennas, high-efficiency antennas have a greater gain. Equation (2.7) gives the mathematical formula for the antenna efficiency (Balanis, 2005).

$$e_0 = e_r e_{cd} = e_{cd}(1 - |\Gamma|^2) \tag{2.7}$$

That(e_0) is the total efficiency, (e_r) is the reflection efficiency, (e_{cd}) is the antenna efficiency, and(Γ) is the voltage reflection coefficient.

2.3.5. Resonant Frequency

In general, an antenna operates in a particular frequency band based on its length. The resonant frequency is the frequency at which the antenna oscillates with its resonance, usually referred to as the middle operational frequency (Balanis, 2005).

2.3.6. Input Impedance

It is the proportion of voltage and current at a pair of antenna terminals or the impedance that the antenna exhibits at its terminals. Equation (2.8) gives the mathematical formula for input impedance (Balanis, 2005).

$$Z_{in} = \frac{V_i}{I_{in}} \tag{2.8}$$

Where Z_{in} is the antenna input impedance (Ohms), V_i antenna input voltage (Volts) and I_{in} is antenna input current (Ampere).

2.3.7. Bandwidth

Another parameter to qualitatively estimate antenna performance is the antenna bandwidth. An antenna's bandwidth is the difference between its high and low frequencies. As shown in Figure 2.7, is generally measured at -10 dB of the antenna's return loss.

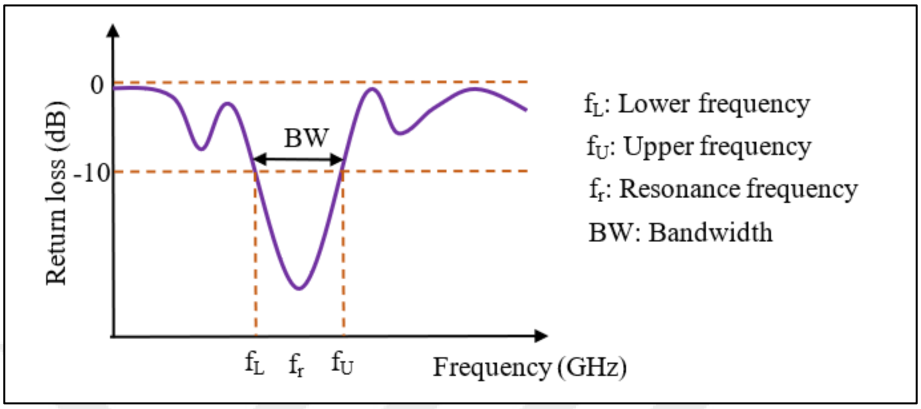

Figure 2.7. Bandwidth Form

2.3.8. Polarization

It is the direction of the electric field radiated from the antenna concerning the Earth’s surface. There are basically three types of polarization: linear, elliptical, and circular, in that the movement of the current in the antenna signifies the type of polarization generated as shown in Figure 2.8.

When the electric fields move along an axis, the polarization is linear. While if the components of the electric fields are equal and the angle between them is 90 degrees, it is called circular polarization. In addition, Elliptical polarization includes linear and circular polarization. Moreover, the wave is called elliptically polarized if the field has two linear and orthogonal components of equal or different magnitudes (Balanis, 2005).

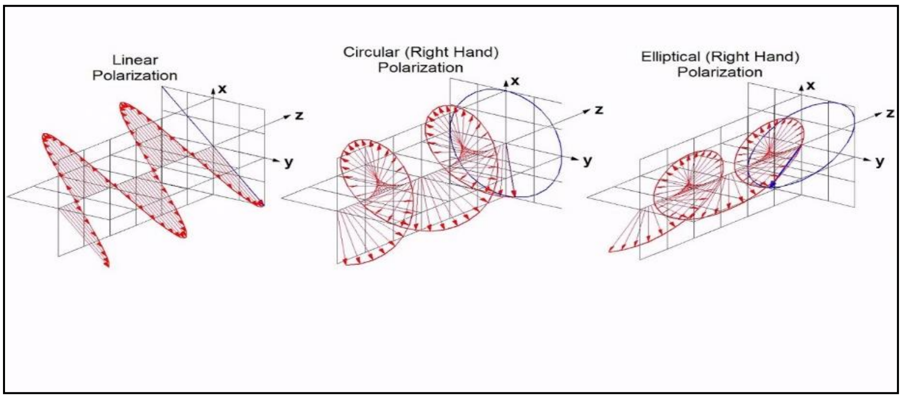

Figure 2.8. Polarization type (Cronin, 2018)

2.3.9. VSWR

VSWR is referred to as the "voltage standing wave ratio". It is the proportion of the highest and lowest limits of voltages. Also, a standing wave is formed as power is reflected from a load. Equation (2.10) gives the mathematical formula for VSWR (Balanis, 2005).

From the impedances, it can be derived the load impedance (Z_L) and the transmission line impedance (Z_O) as both are used to compute Γ "the voltage reflection coefficient near the load" as shown in equation (2.9).

$$\Gamma = \frac{(Z_L - Z_O)}{(Z_L + Z_O)} \tag{2.9}$$

$$\mathrm{VSWR} = \frac{(1+|\Gamma|)}{(1-|\Gamma|)} \tag{2.10}$$

2.3.10. Return Loss

It is a main parameter for measuring the compatibility between the antenna and the transmitter (Balanis, 2005). It also determines how efficiently an antenna delivers power to a source and as shown in Figure 2.9 it is measured in dB. Also, return loss can be calculated as shown in equation (2.11) below.

$$\mathrm{RL} = -20\log_{10}|\Gamma| \tag{2.11}$$

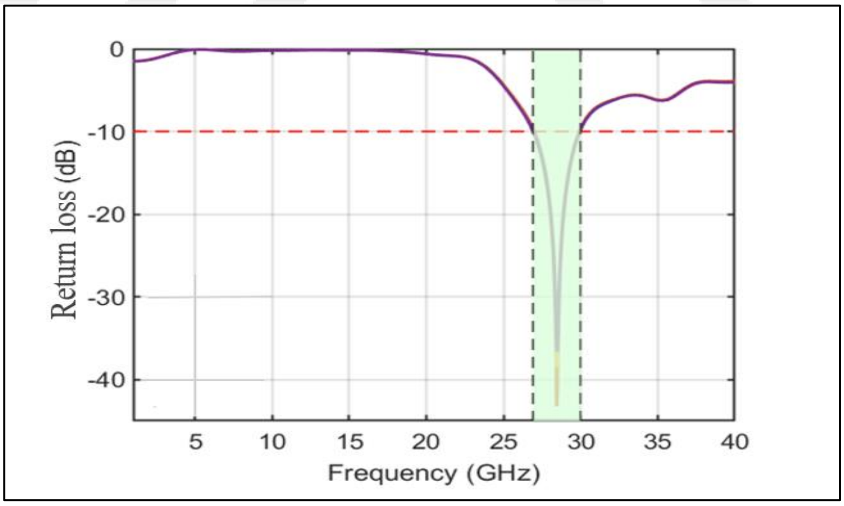

Figure 2.9. Resonance frequency at 28 GHz return loss

2.4. The Fifth Generation

Wireless communications technology has changed the way we communicate in remarkable ways since its inception. It has helped us transmit data over a distance without wires. The evolution of wireless communication started with the first generation and has progressed to the fifth generation. Each generation is an old, improved version and each new generation offers higher speeds, greater capacity, and more features as shown in Figure 2.10. Initially, the first generation (1G) was analog cellular support for mobile voice calls but it was limited in terms of coverage and capacity. The second generation (2G) introduced digital cellular support and it was able to support up to 270 kbps data rate. With the third generation (3G), data rates can reach 14.4 Mbps, which is sufficient to support video calling. While the fourth generation (4G) has much higher data rates, up to 1Gbps (Adachi et al, 2002).

Because of the incredibly high number of connected devices and the lack of bandwidth, 5G has been introduced. This introduction of 5G marks an important milestone in the 21st century. This can help provide high resolution and large bandwidth in gigabits.

5G technology increases data rate and bandwidth, reduces battery consumption, improves coverage, and addresses latency, security, reliability, and cost issues. Furthermore, one of the main issues in 5G communications is spectrum allocation (Osseiran et al, 2014).

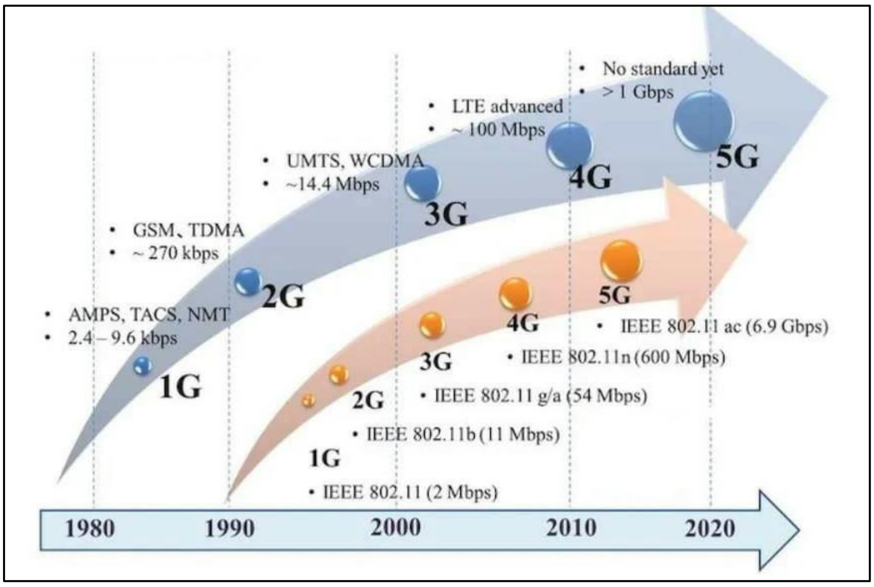

Figure 2.10. Mobile wireless evolution (Surantha et al, 2017)

2.4.1. The Frequency Bands of 5G

The fifth generation identifies different frequency bands as shown in Figure 2.11.

(FR1: 410 - 7125 MHz) which is named sub-6 GHz.

(FR2: 24 -52 GHz) which is named millimeter-wave.

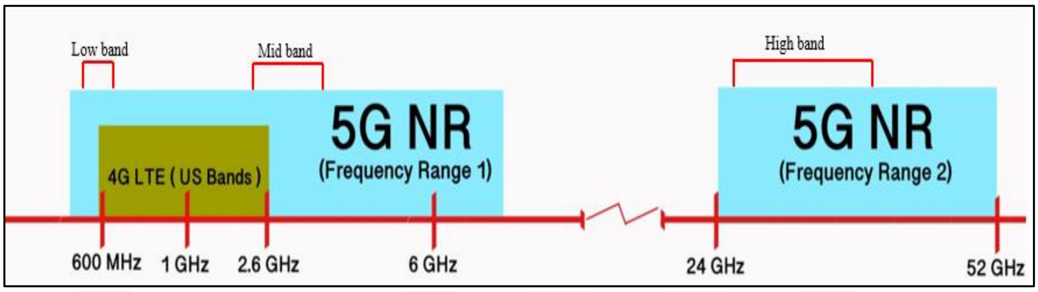

Figure 2.11. 5G frequency bands

As shown in Figure 2.12, the spectrum consists of four frequency bands (low, mid, and high). Bands differ in capability: low bands (less than 1GHz) offer greater coverage, mid bands (1 GHz–6 GHz) offer a balance of speed and coverage while high bands (24 GHz–40 GHz) provide higher speeds but smaller coverage zones (5G spectrum bands explained, 2020).

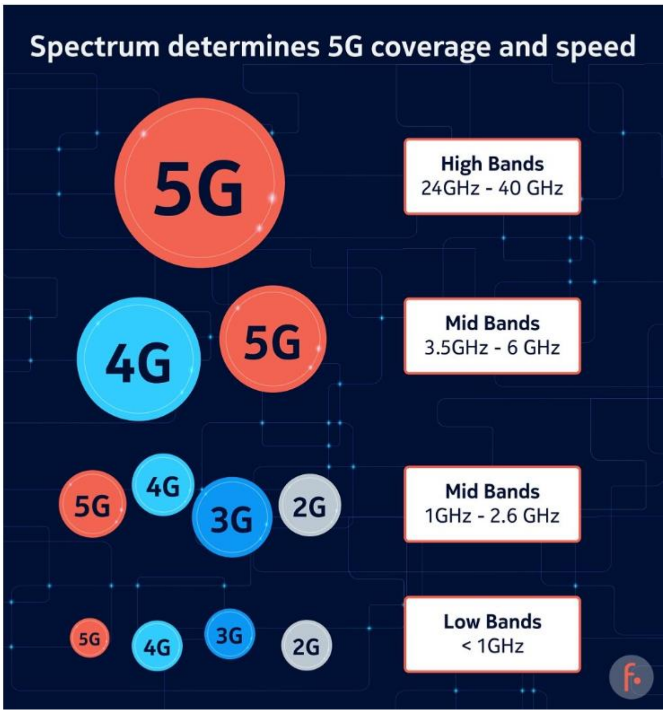

Figure 2.12. Spectrum coverage of 1G, 2G, 3G, 4G, and 5G (5G spectrum bands explained, 2020).

Figure 2.13 illustrates several characteristics of each frequency spectrum, such as low latency, wide range, and sensing accuracy, among others. 2G/3G offers high coverage and low latency, In contrast, 6G offers low coverage, high latency, and high sensing accuracy, with wide bandwidth. Further, both types of 5G have more good features than 4G.

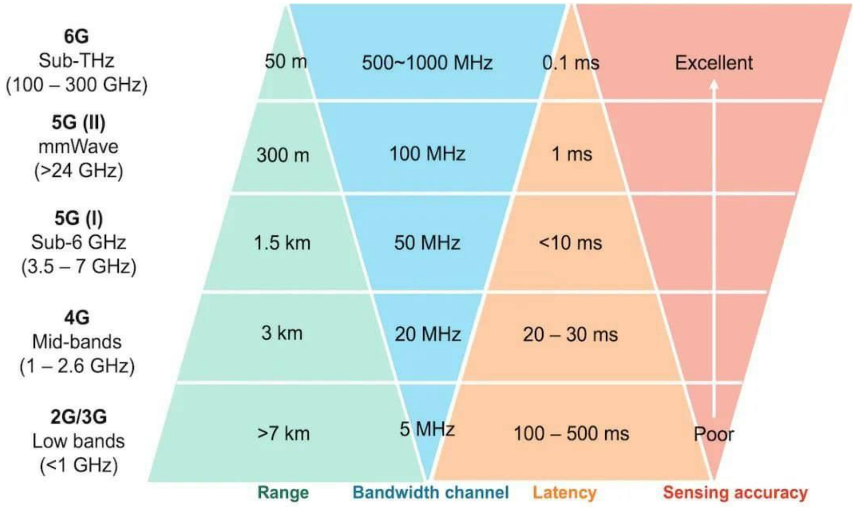

Figure 2.13. Features of different frequency bands (Embedded Computıng (Desıgn, 2021)

In terms of mobile wireless communications, 5G has several advantages as follows.

- There is a rapid increase in mobile data traffic.
- The rapid increase in connected devices.
- Improves coverage, and addresses latency, security, reliability, and cost issues.
- It provides more energy efficient for both mobile devices and networks.
- 5G offers improved operational performance (higher data rates and spectral efficiency).

2.5. Millimeter-Wave

As technology develops, user demands increase. Therefore, more bandwidth should be made available to meet user demands. 5G mobile communications standard recognizes the need for millimeter-wave frequency bands. mm-Wave has shown great potential for increasing wireless data rates due to its high bandwidth.

As shown in Figure 2.14, mm-wave frequencies range from 30 to 300 GHz. The unused mm-wave spectrum offers an excellent opportunity for additional broadband capacity and thus better quality of service for users (Rangan et al, 2014).

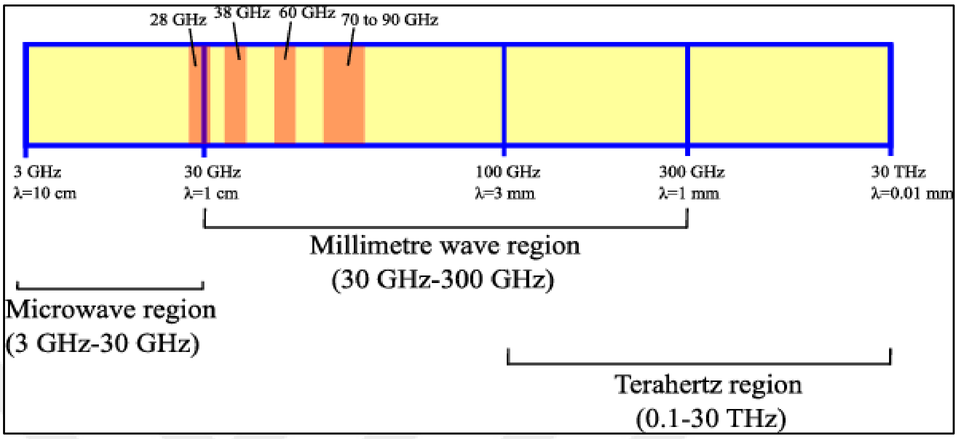

Figure 2.14. Millimeter-wave frequencies (Lawrence et al, 2017)

In terms of mobile wireless communications, millimeter-wave has several advantages over sub-6GHz wireless technologies that make it a strong contender for the future (Rappaport et al, 2013).

- Provides wide bandwidth and thus more subscribers can be accommodated.
- The size of millimeter-wave components is small. As a result, millimeter-wave systems are easier to miniaturize.
- Up to 400 meters of backhaul are supported by the 5G millimeter-wave networks.
- With 5G millimeter-wave networks, you can transmit data at a higher rate, utilize spread spectrum, and be more resistant to interference.

However, despite the above attractive advantages, millimeter-wave also has some disadvantages.

- As mm-waves travel through the atmosphere, they are subject to a variety of losses, including penetration and rain attenuation.

- There is significant attenuation at extremely high frequencies. Therefore, an mm-wave is not suitable for long-distance communication.

- The millimeter-wave frequency consumes more power.

2.6. Standards of 5G mm-Wave Frequency Bands

The frequency bands used by 5G depend on the country of use. Unlike the traditional lower bands found worldwide, other higher bands vary. Frequency bands can be specific to a country or a selected group of countries (5G Frequency Bands, 2022).

The third generation partnership project (3GPP) standard has selected the frequencies of 28 and 38 GHz as the Ka-band which has four standard support in different countries as shown in Figure 2.15.

The standard (n257) covers a broad range from 26.5 to 29.5 GHz for the U.S., Japan, and South Korea. While the standard (n261) is a subset of the band (n257) and covers a narrower range from 27.5 to 28.35 GHz. Whereas the standard (n258) for Europe and China covers from 24.25 to 27.5 GHz. Also, the standard (n260) for the U.S. covers from 37 to 40 GHz.

In addition, there are three other V-band standards. (n259) covers 39.50 – 43.50, (n262) covers 47.20 – 48.20, and (n263) covers 57.00 – 71.00.

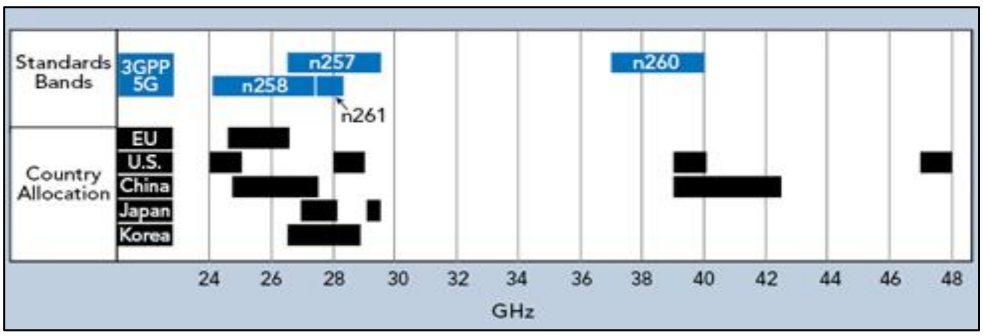

Figure 2.15. 5G mm-wave frequency bands (Microwave Journal, 2019)

Several factors make 28 / 38 GHz among the existing mm-Wave the most suitable millimeter-wave frequencies for 5G (Al-Falahy and Alani, 2019).

- The ka-band has been the subject of much research about the 5G mobile communications standard.
- Having a wide bandwidth is necessary for a high data rate on the high-frequency band.
- Spectrum Availability as many of the spectrum bands is underutilized, allowing several hundred megahertz to be assigned to 5G services.
- In terms of geographic harmony, the ka-band is available in the greatest number of countries.
- Since these bands are less affected by atmospheric absorption and attenuation, they are advantageous for cellular communications as shown in Figure 2.16 below.

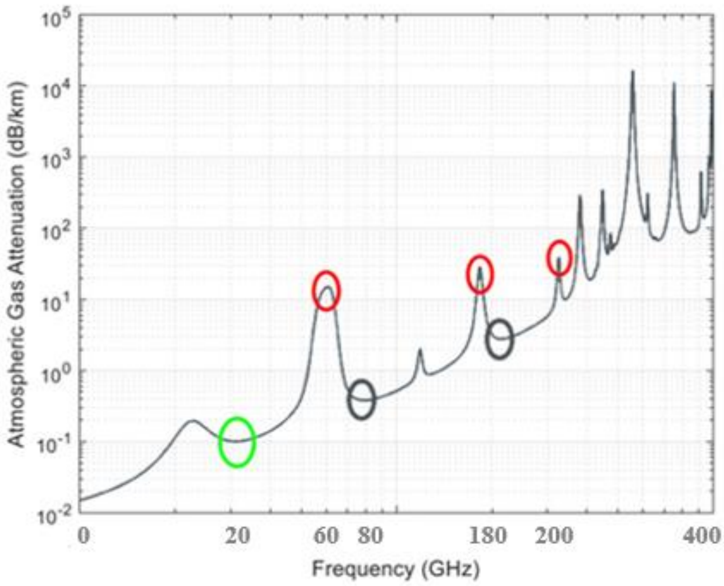

Figure 2.16. Atmospheric attenuation across an mm-wave band (Rangan et al, 2014).

2.7. MIMO System

MIMO is a crucial component of modern telecommunications technology. MIMO uses multiple antennas for wireless communication at both the senders and receiver as depicted in Figure 2.17. MIMO communication uses a single radio channel to simultaneously transmit the same information as multiple signals over multiple antennas. As a result of multipath propagation with MIMO antennas, the key features of 5G such as data rates, capacity, and connection reliability all rise. Additionally, MIMO uses waves bouncing off existing obstacles to providing a better signal even if the device is not in the line of site. Multiple components of MIMO enable multiple data rates and reduce packet loss. MIMO is a key factor in reducing antenna space for mobile phones (Everything RF, 2019).

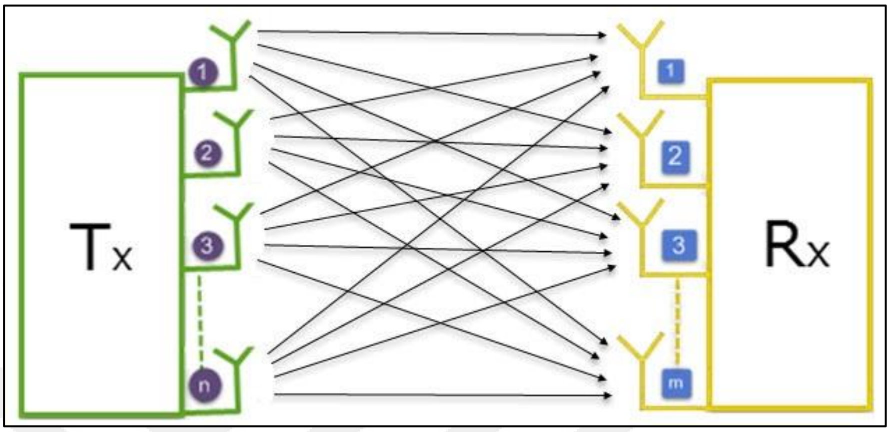

Figure 2.17. MIMO system (Everything RF, 2019).

MIMO comes in many sizes, (n × m) MIMO means n antennas work as senders and m as a receiver.

2.7.1. Performance Parameters of MIMO

The MIMO antenna performance can be determined through the ECC and DG (Khalid et al, 2020).

2.7.1.1. Envelope Correlation Coefficient

It is classified as a crucial element of MIMO performance, which indicates how well the antenna elements are coupled. ECC can be computed between every two ports of the antenna as explained in the equation (2.12) (Sharawi, 2013).

$$\rho_{eij} = \frac{|S_{ii} * S_{ij} + S_{ji} * S_{jj}|^2}{(1-|S_{ii}|^2 - S_{ij}{}^2)(1-|S_{Ji}|^2 - S_{Jj}{}^2)} \qquad (2.12)$$

Where (ρ_{eij}) stands for envelope correlation coefficient while the (S_{ij}) stands for the S parameter of the ith and jth ports.

2.7.1.2. Diversity Gain

It is "the loss in transmission power when diversity schemes are applied on the component". To compute diversity gains, the formula (2.13) is used (Sharawi, 2013).

$$DG = 10\sqrt{1 - |\rho_{eij}|^2} \tag{2.13}$$

3. MATERIALS AND METHODS

In this section, a brief overview of software and hardware requirements that are necessary for designing the antenna as well as the steps involved in the construction of the 5G MIMO antenna was discussed.

3.1. Software Requirements

CST studio is a high-performance 3D analysis software package for the design, analysis, and optimization of electromagnetic systems as shown in Figure 3.1. A simulation uses a model of a real system in the form of a computer program. High-frequency devices such as antennas, filters, and couplers can be analyzed quickly and accurately using this software. In addition, the CST studio suite makes a significant contribution to displaying virtual prototyping before physical experiments (Rescale, 2022).

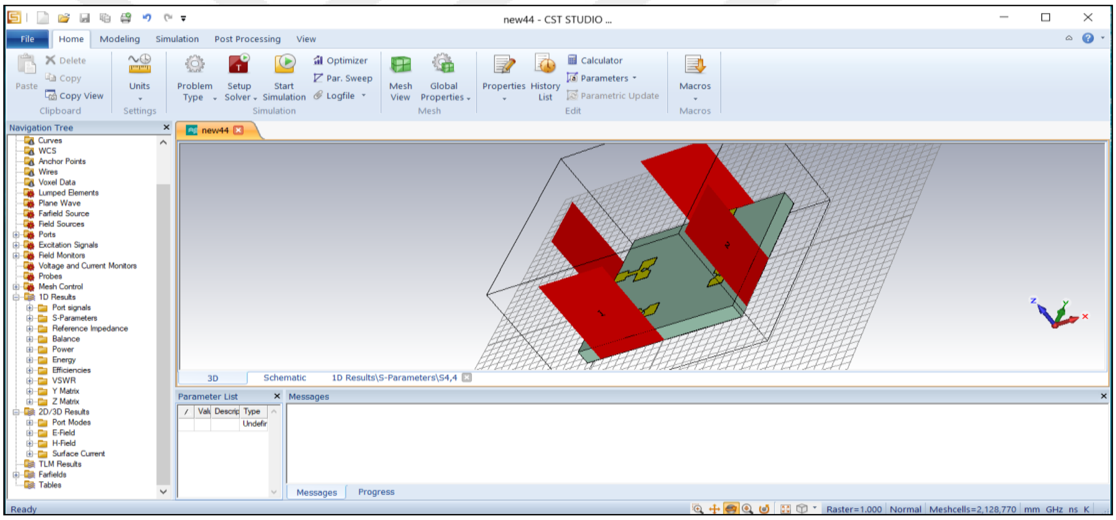

Figure 3.1. CST program

3.2. Hardware Requirements

The "FR-4" name refers to the dielectric material’s flame-retardant qualities as well as the type-4 woven glass-reinforced epoxy laminate utilized in its manufacturing. FR-4 is the most popular dielectric material used in the production of printed circuit boards. FR-4 has some advantages, such as low cost and is easily available. FR-4 is not only strong and water resistant, but it also provides superior insulation between copper layers and maintains signal integrity while minimizing noise (Hiçdurmaz and Gümüşm, 2019).

Copper is a metal that is easily shaped into sheets and wires. Copper is a highly conductive metal. The majority of its applications are based on this feature or the fact that it is also a good thermal conductor. Copper is also twice as conductive as aluminum, making it an ideal choice for antenna material (Hiçdurmaz and Gümüşm, 2019).

Table 3.1. Characteristics of the hardware material

	Permittivity Ɛ (F/m)	Permeability μ (H/m)	Conductivity σ (S/m)
FR-4	4.4	1.0	-
Copper	1	1.0	58×10^6

SMA is the standard male connector. SMA connectors have an impedance of 50 Ω. Also, it is a type of screw-type coaxial connector usually used in microwave systems and mobile telephone antennas as shown in Figure 3.2.

Figure 3.2. Standard connector SMA (Connector supplier, 2022)

3.3. Antenna Design

An antenna with a compact size and wide bandwidth that provides high gain, low return loss, and low return loss is an important design challenge. Computer simulation software is used to simulate the antenna. CST is an essential device for replicating devices at high repetition rates in 3D and the market leader for time domain replication. Using it, you can study radio channels, links, couplers, multilayer structures, signal integrity, and electromagnetic compatibility quickly and accurately. A patch antenna is one of the most significant components. A microstrip patch antenna has the advantages of being small, low-profile, easy to manufacture and integrate, and affordable over other types of antennas. Also, when designing a microstrip patch antenna, impedance matching should be accurate, microstrip inset feed lines are used to provide the antenna with a source, and For the analysis of microstrip antenna, there are several methods such as "the transmission line model, cavity model, and full wave mode". As a popular and simplest method among the above-mentioned models, we have used transmission-line mode. The antenna design process involves designing the radiator patch and feed line. The design of a microstrip antenna requires three parameters: the dielectric constant (ε_r), the thickness of the substrate (h), and the resonant frequency (f_r), which have a significant influence on antenna characteristics (Balanis, 2005).

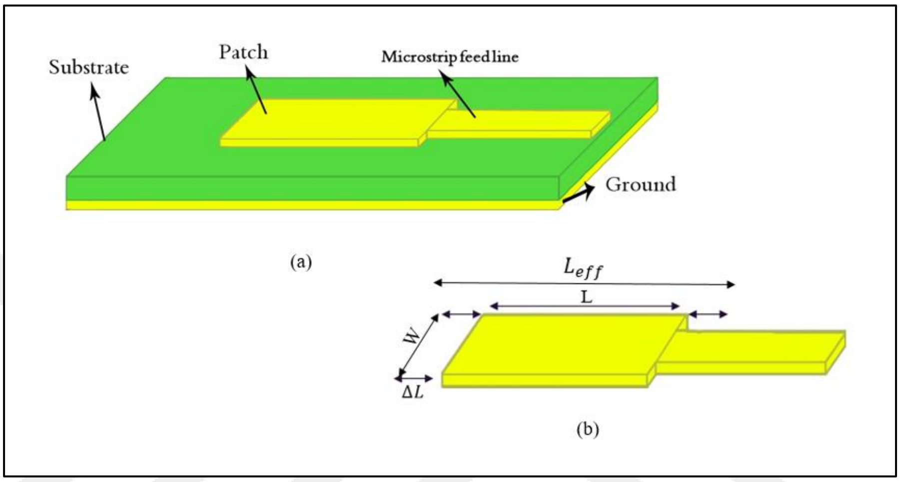

Figure 3.3. a) Microstrip antenna, b) Top view of the antenna

According to equation (3.1), the width of the antenna is determined, as the c value is 3×10^8.

$$W = \frac{c}{2f_r\sqrt{\frac{(\varepsilon_r+1)}{2}}} \quad (3.1)$$

According to equation (3.2), the effective permittivity is determined.

$$\varepsilon_{eff} = \frac{1}{2}(\varepsilon_r + 1) + \frac{1}{2}(\varepsilon_r - 1)(1 + 12\frac{h}{w})^{\frac{-1}{2}} \quad (3.2)$$

According to equation (3.3), the extension length is calculated.

$$L_{eff} = \frac{c}{2f_r\sqrt{\varepsilon_{eff}}} \quad (3.3)$$

According to equation (3.4), we can calculate the extension length caused by the fringing field.

$$\Delta L = 0.412h\frac{(\varepsilon_{eff}+0.3)(\frac{W}{h}+0.264)}{(\varepsilon_{eff}-0.258)(\frac{W}{h}+0.8)} \tag{3.4}$$

According to equation (3.5), The length of the patch is determined.

$$L = L_{eff} - 2\Delta L \tag{3.5}$$

As the substrate for this design, FR-4 was chosen for two reasons: first, it was easily available, and second, it has a low loss factor. It has a dielectric constant of 4.4, a height of 1.55 mm, and a dielectric loss tangent of 0.02. Additionally, the patch conductor and ground plane are copper, and both are 0.035 mm thick. Also, it is fed through an SMA connector 50 Ω. According to equations (3.1), (3.2), (3.3), (3.4), and 3.5, the length of the patch and the width is specified.

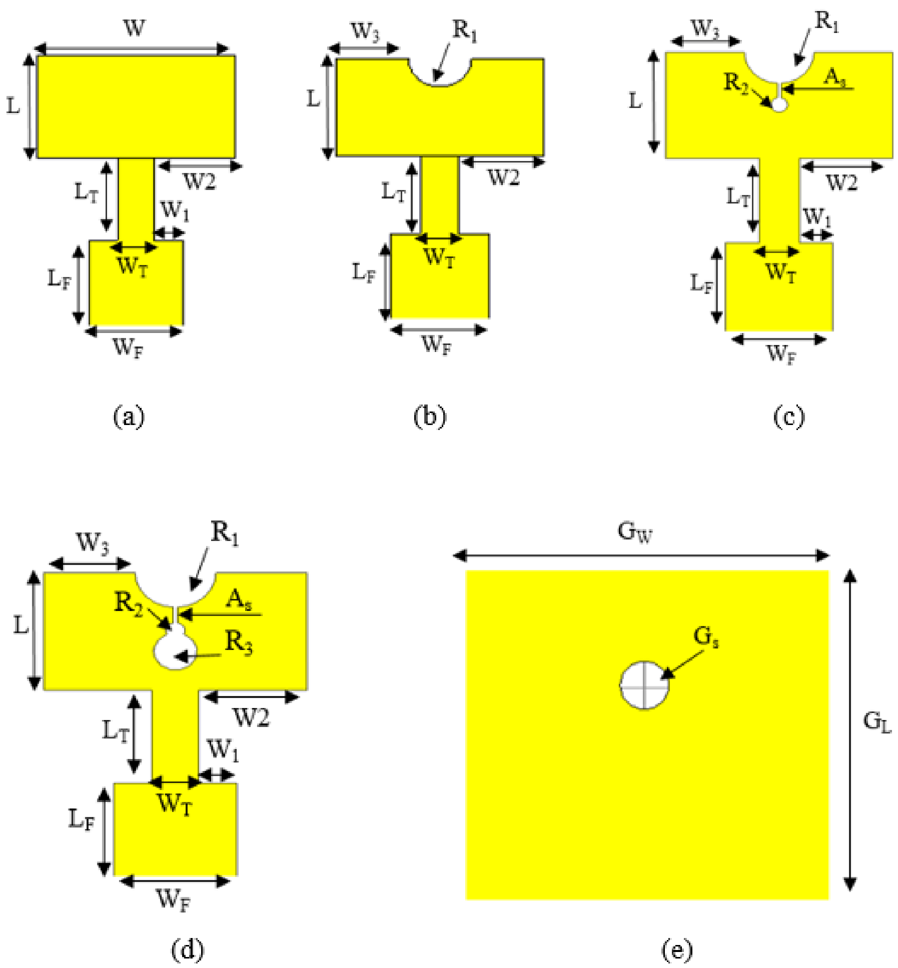

Figure 3.4. A step-by-step for designing the single antenna a) phase 1, b) phase 2, c) Phase 3, d) phase 4, e) Ground is the same for b and c phases

Table 3.2. A single antenna's dimensions

Parameter	Dimensions [mm]	Parameter	Dimensions [mm]
L	2.16	W	3.26
L_T	1.35	W_T	0.58
L_F	1.47	W_F	1.53
W_1	0.47	W2	1.34
W_3	1	R_1	0.63
R_2	0.2	R3	0.35
A_s	0.1 x 0.23	G_s	0.63
G_L	8.75	G_W	8.75

As can be seen in Figure 3.4 above, numerous procedures were applied to the rectangular patch antenna to improve its parameters. These procedures included the addition and constant modification of up to four slots on the patch antenna and one slot on the ground, respectively. Once the last design of the antenna, with the most satisfactory characteristics, was achieved, the 5G MIMO antenna was constructed by implementing four identical elements arranged circularly with 18 x 18 mm overall size in which they have minimal interference with each other.

Figure 3.5 illustrates the initial design of the MIMO antenna which was then developed to comply with the U.S. standard (26.5 to 29.5 GHz) as illustrated in Figure 3.6.

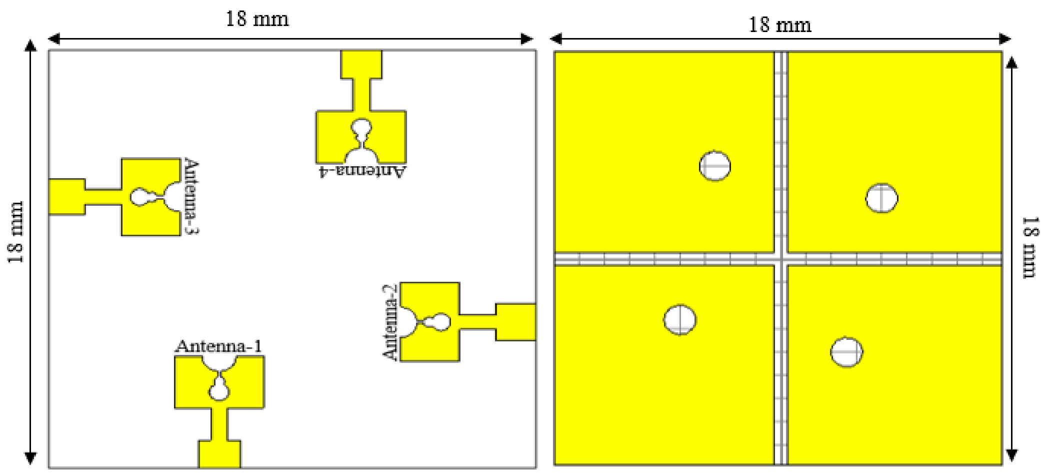

(a) (b)

Figure 3.5. a) front, b) back side of the first suggested MIMO

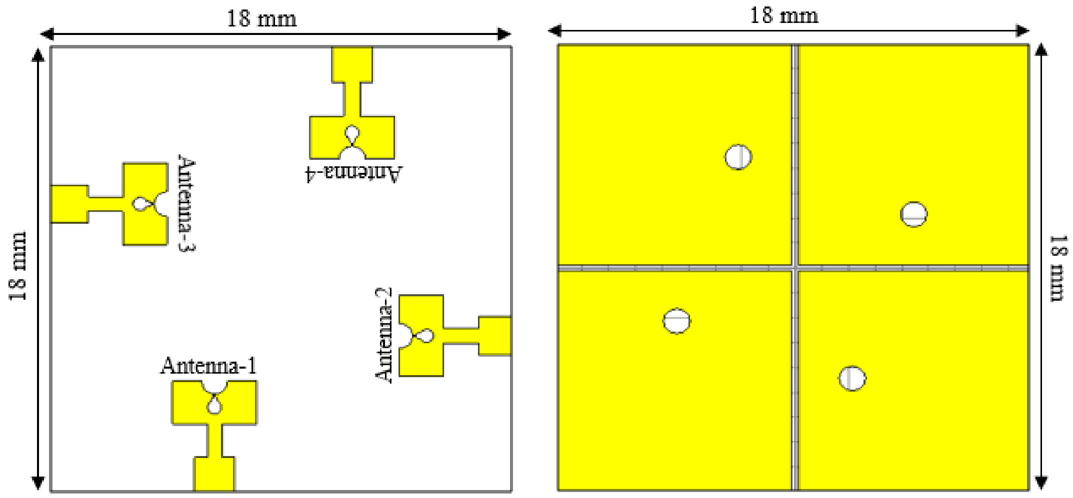

(a) (b)

Figure 3.6. a) front, b) back side of the second suggested MIMO

As noticed that the size of the slot in the ground and its place, the space between each antenna patch, the length and the width of the ground and the length of the patch antenna have a great impact on matching the operating frequency with the U.S. standard (26.5 to 29.5 GHz).

4. RESULTS AND DISCUSSION

In this chapter, the steps that led to the final result of the single antenna, operating in the desired frequency range, were discussed. Also, the obtained antenna parameters for both proposed MIMO antennas were presented to demonstrate how sufficiently our antennas work. Additionally, all designed antennas were simulated and studied in CST.

4.1. The result of the single antenna

Figure 4.1 depicts the single antenna which is designed in stages to reach the final design. In stage 1, the initial design is presented and the propagation band needs to be modified. In stage 2, the design has been modified by adding a slot in the middle. A similar slot has been added to the back in stage 3, and the results have been good. As the implementation of the slot showed promising results, another three slots were implemented in the middle of the patch. Overall, the adjustments of the slots managed to make the single antenna operate from 25 to 29 GHz and from 34 to 41 GHz based on -10 dB, as a return loss.

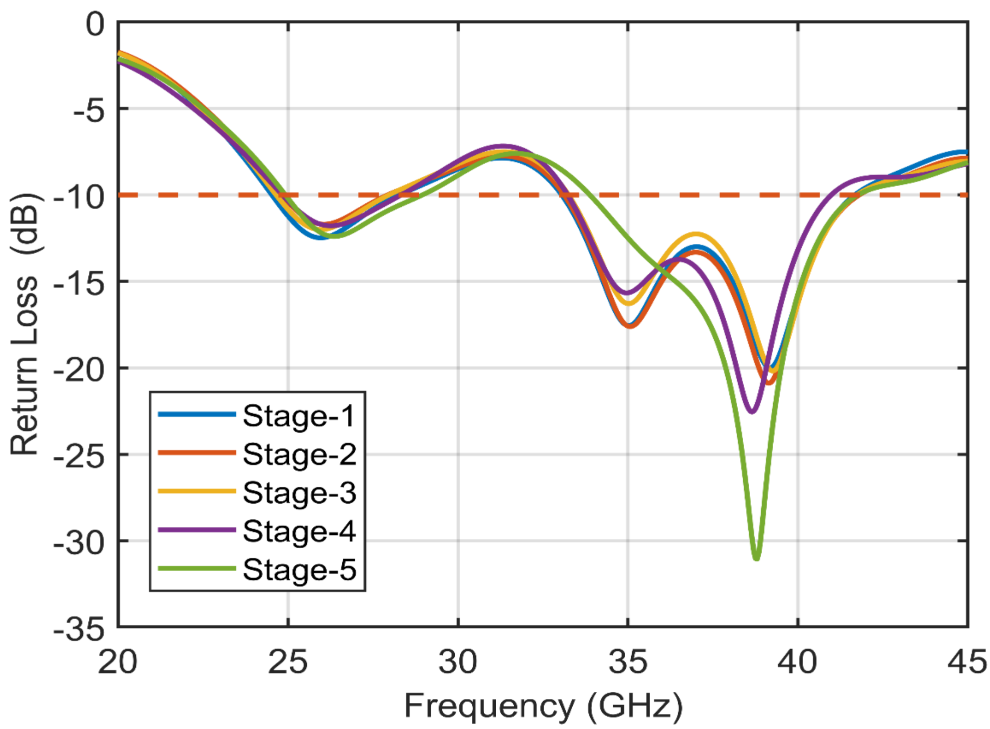

Figure 4.1. A single antenna design's return loss for each stage

4.2. The result of the first designed MIMO antenna

Figure 4.2 illustrate the return loss of each element. From the diagram, it is clear that they all propagate in the dual band and differ minimally regarding the return loss. The first MIMO has a bandwidth of 5.5 GHz with a return loss value of -26 dB at 26 GHz, while at 38 GHz, its bandwidth is 4.5 GHz and has a return loss value of -41 dB.

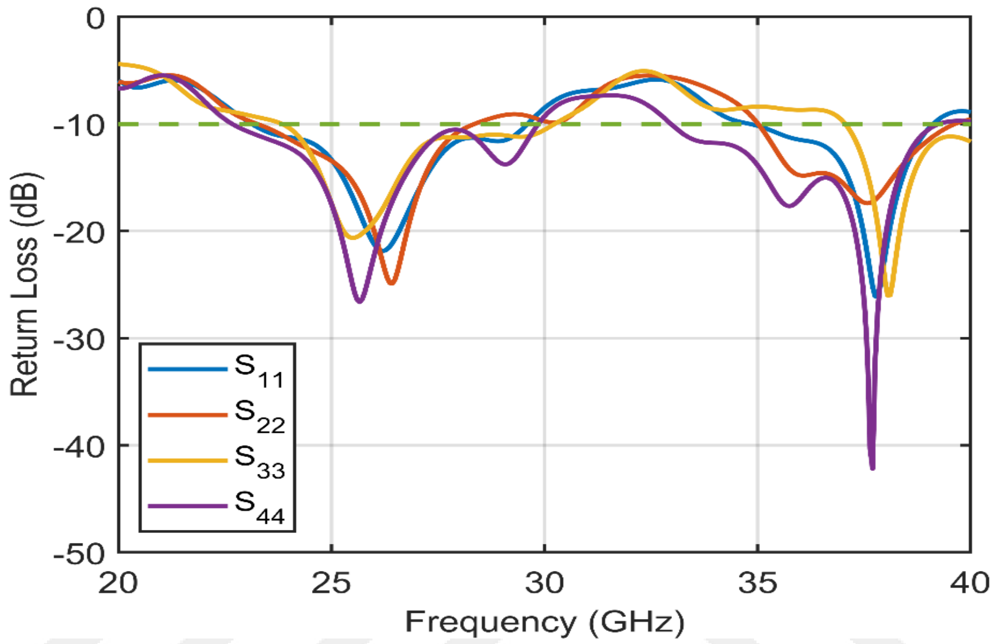

Figure 4.2. Each port's return loss of the first MIMO antenna

Figure 4.3 depicts the isolation between the radiating patches. From the diagram, it is clear that the average isolation at 26 GHz and 38 GHz is below -20 dB and -30 dB, respectively. This is due to the arrangement of the patches in a way that ensures low mutual coupling.

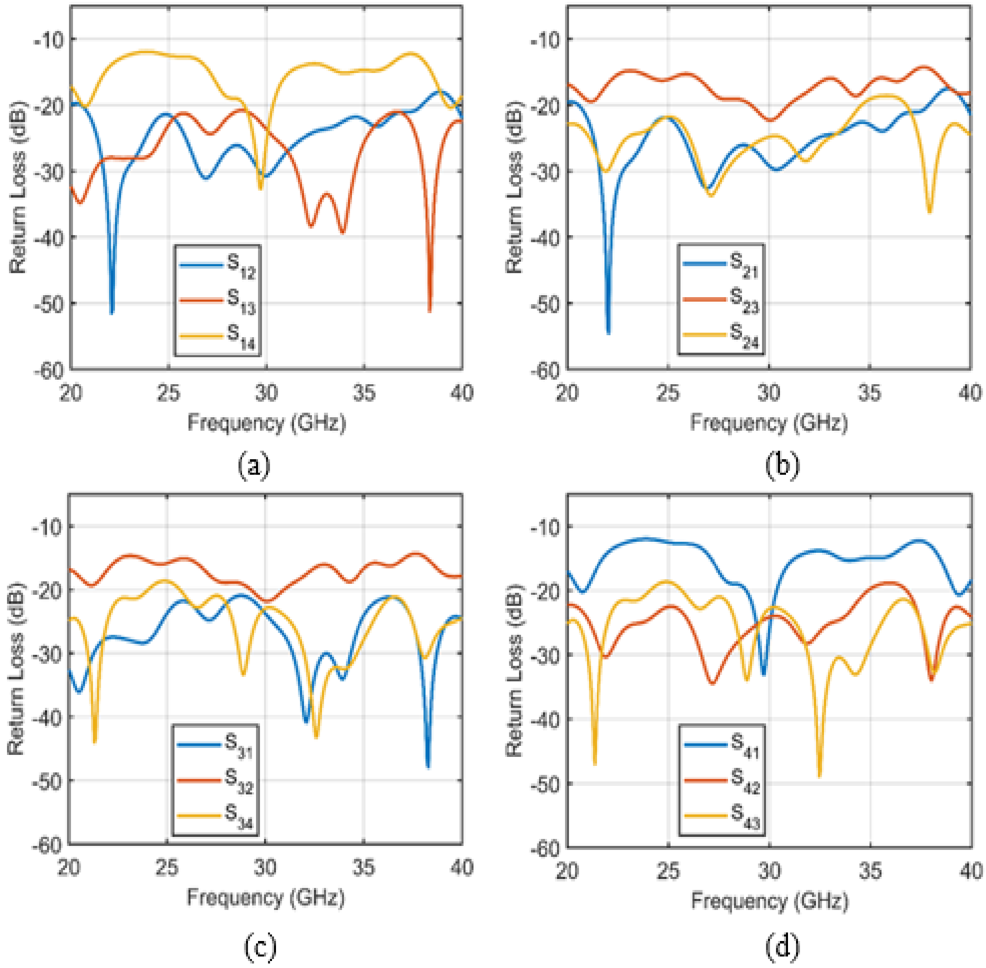

Figure 4.3. Port's isolation between each patch antenna of the first MIMO

One of the significant features of a communication system is the behavior of an antenna in the far region. At 26 GHz, Figure 4.4 illustrates the 3D simulated radiation for each antenna element, and it shows a directional gain of the highest value 9.68 dBi. Whereas Figure 4.5 displays the radiation pattern in the polar form and it shows that a) and d) have a main lobe magnitude of 9.14 dBi while b) and c) have a main lobe of 6.96 dBi and almost all elements show a directional pattern.

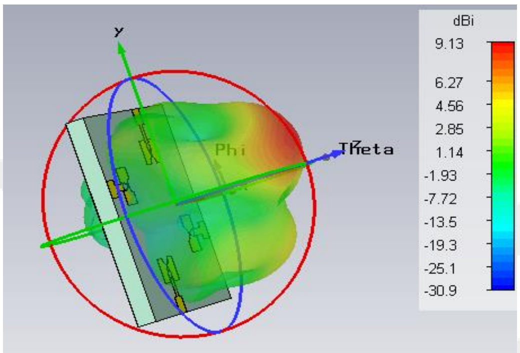

(a)

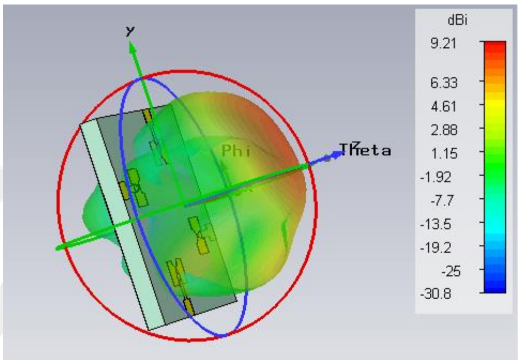

(b)

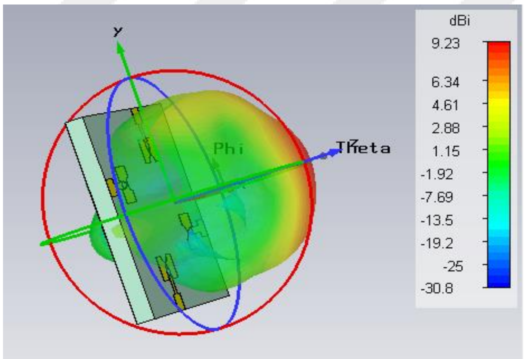

(c)

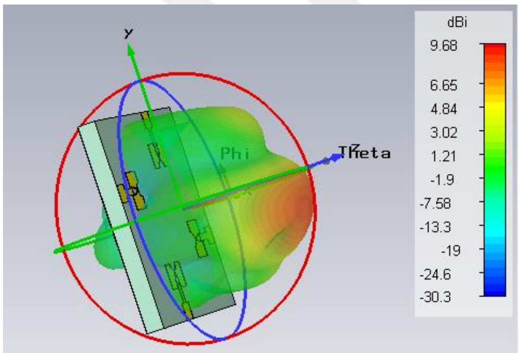

(d)

Figure 4.4. The 3D-dimensional radiation pattern at 26 GHz of a) port 1, b) port 2, c) port 3, d) port 4

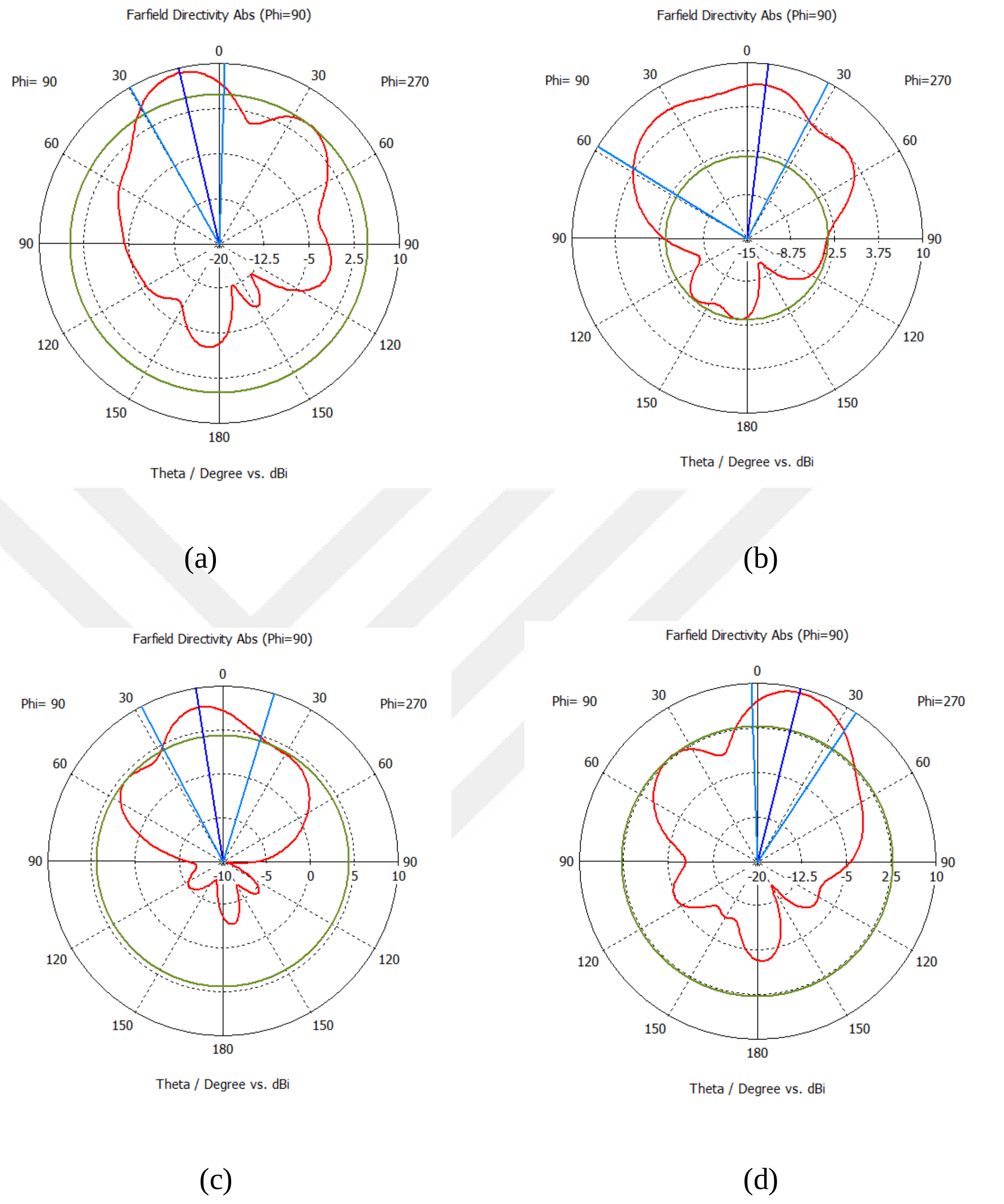

Figure 4.5. The polar radiation pattern at 26 GHz of a) port 1, b) port 2, c) port 3, d) port 4

At the second frequency (38 GHz), the 3D simulated radiation patterns of the first MIMO antenna for each antenna element is shown as a directional gain of the highest value 6.71 dBi in Figure 4.6. Whereas Figure 4.7 displays the radiation pattern in the polar form and it shows that each port has a different main lobe magnitude of a) 5.33 dBi, b) 4.61 dBi, c) 2.77 dBi, and d) of 3.6 dBi, and almost all elements show a semi-directional pattern.

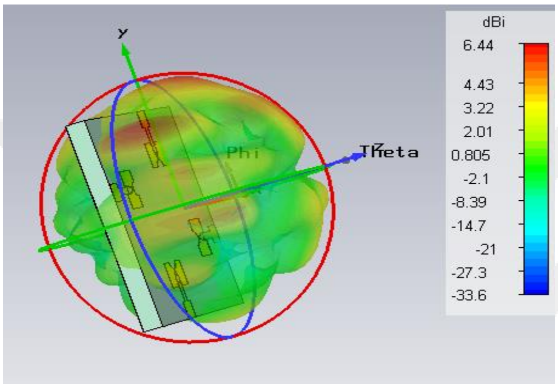

(a)

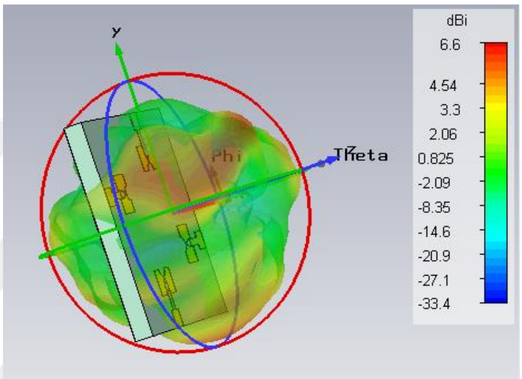

(b)

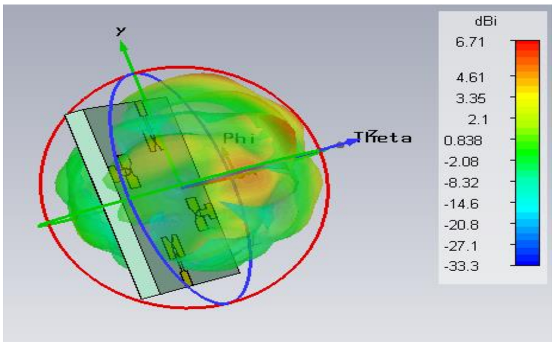

(c)

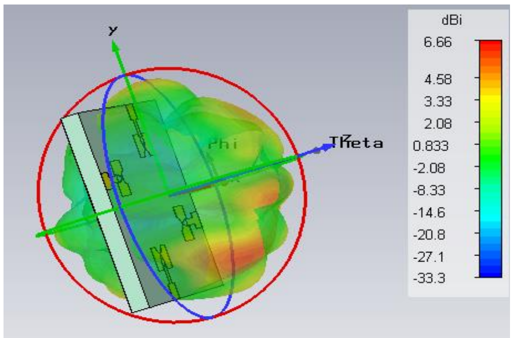

(d)

Figure 4.6. The 3D-dimensional radiation pattern at 38 GHz of a) port 1, b) port 2, c) port 3, d) port 4

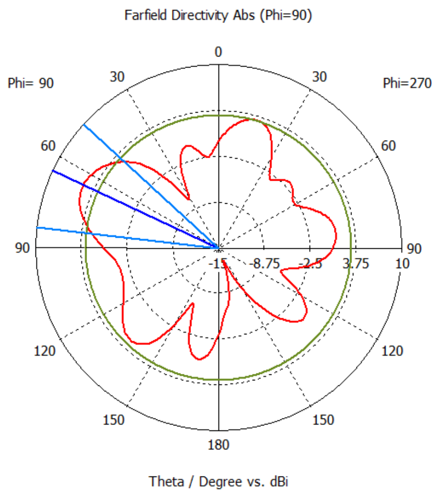

(a)

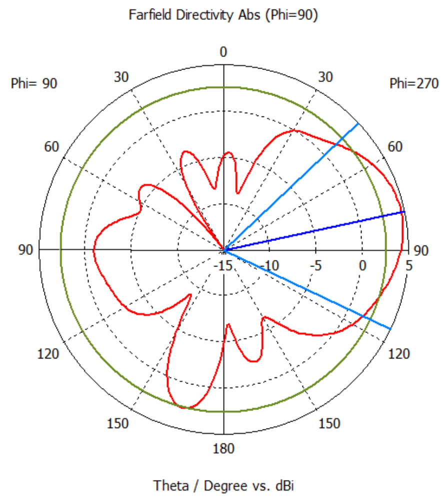

(b)

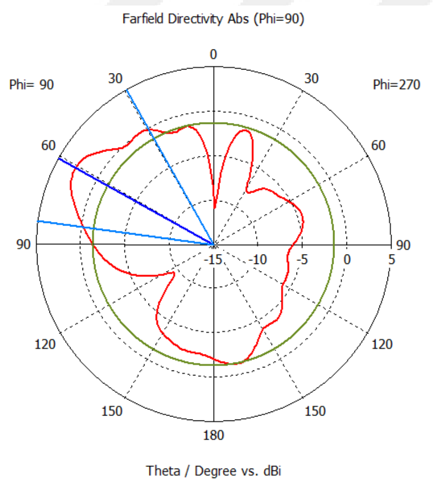

(c)

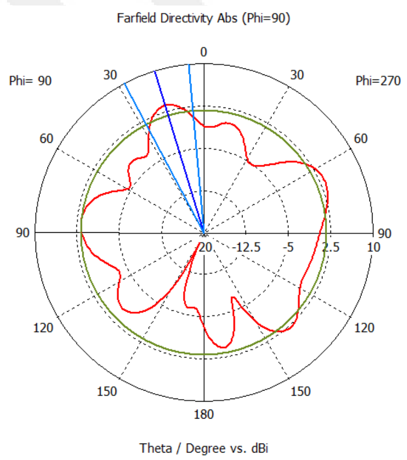

(d)

Figure 4.7. The polar radiation pattern at 38 GHz of a) port 1, b) port 2, c) port 3, d) port 4

The efficiency of each element of the designed MIMO antenna is clarified in figure 4.8. The total efficiency at 26 GHz is higher than 60% whereas at 38 GHz is higher than 50% for all ports.

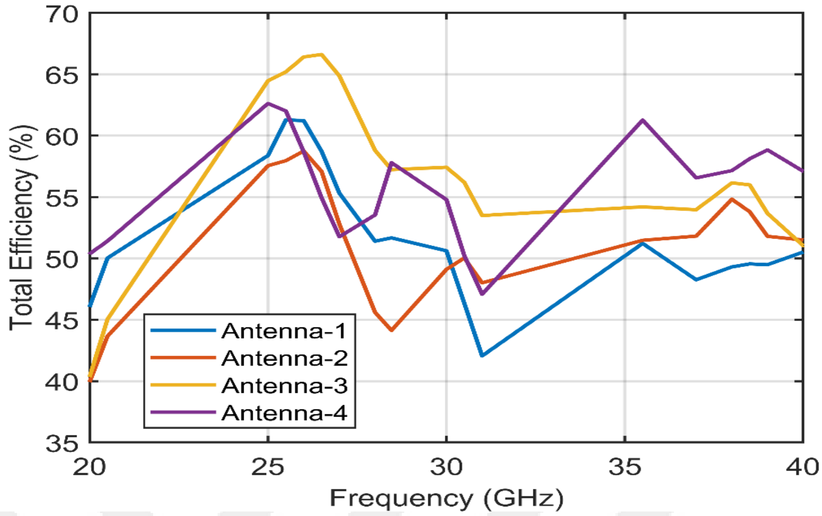

Figure 4.8. Antenna efficiency of each port of the first MIMO antenna.

Several factors influence MIMO antenna performance, but mainly the ECC. Figure 4.9, displays the ECC between each port at the desired bands for the proposed MIMO antenna. Additionally, Table 4.1 provides each ECC value between each port at 26 GHz and 38 GHz.

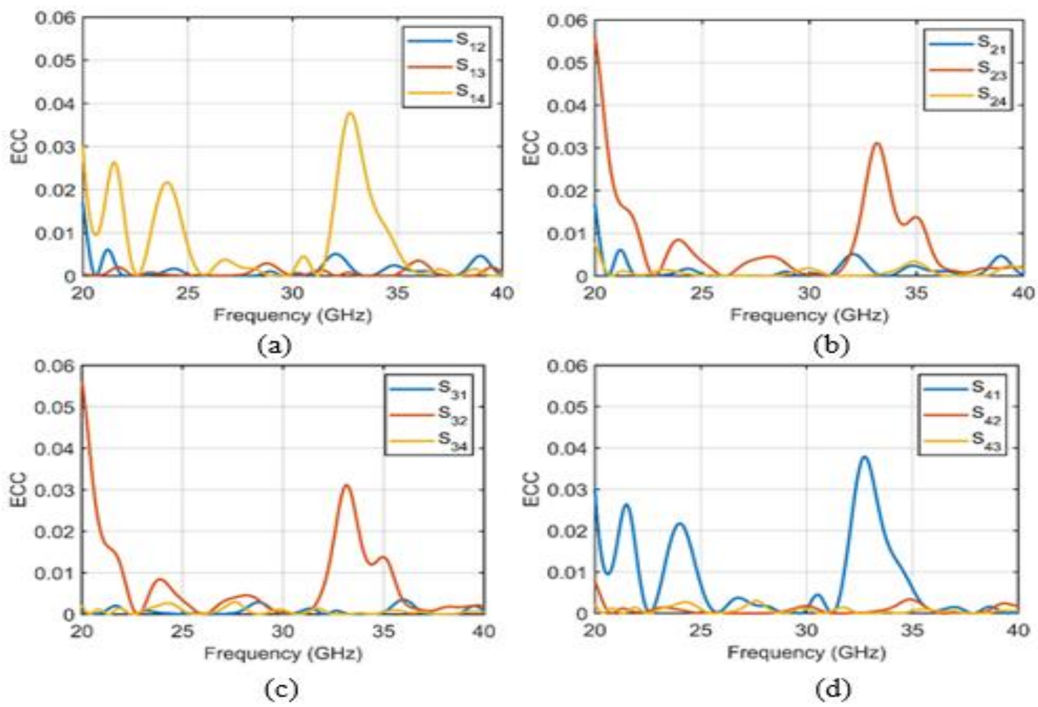

Figure 4.9. The ECC performance for the first designed MIMO antenna

Table 4.1. Port's ECC value between each patch antenna of the first MIMO

ECC	26 GHz	38 GHz
S_{12} / S_{21}	5.8665×10^{-5}	0.0007
S_{13} / S_{31}	0.002	4.82×10^{-6}
S_{14} / S_{41}	0.0006	0.007
S_{23} / S_{32}	3.37×10^{-5}	0.00173
S_{24} / S_{42}	6.5×10^{-5}	3.34×10^{-5}
S_{34} / S_{43}	0.000156	1×10^{-5}

Likewise, another key performance metric is the diversity gain, which illustrates the "loss in transmission power when diversity schemes are applied on the component". In Figure 4.10, it can be seen that the DG is close to 10 dB at the desired frequency bands (26 and 38 GHz).

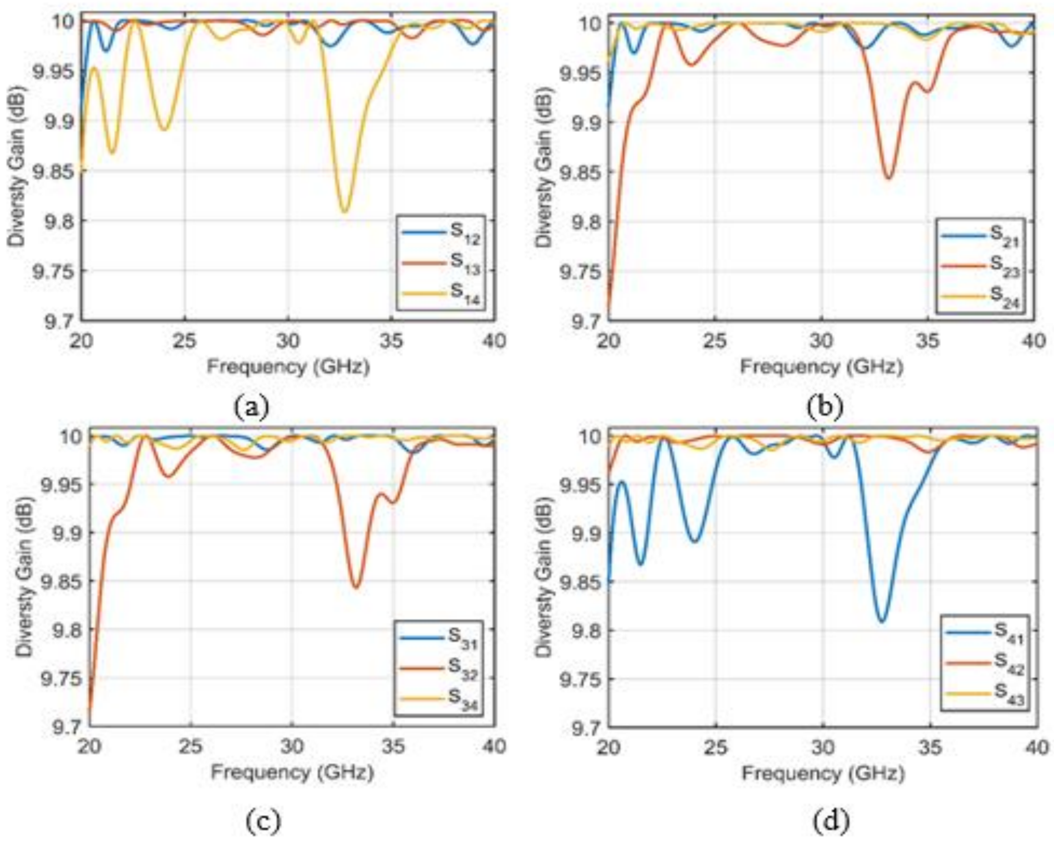

Figure 4.10. The DG performance for the first designed MIMO antenna

Fig. 4.11 and Fig. 4.12 illustrate the distribution of the surface current of the first designed MIMO antenna regarding each patch in the band of 26 GHz and 38 GHz, respectively. Accordingly, the current intensity across the connecting strips of the circular slots in the center of the patch is high. Thus, the slot and the connecting strips with the feed contribute more to mm-wave band attainment. Furthermore, the surface current distribution pattern also indicates that the interference between patches is negligible. Since each patch has arranged in a way that makes it 90 degrees away from the other.

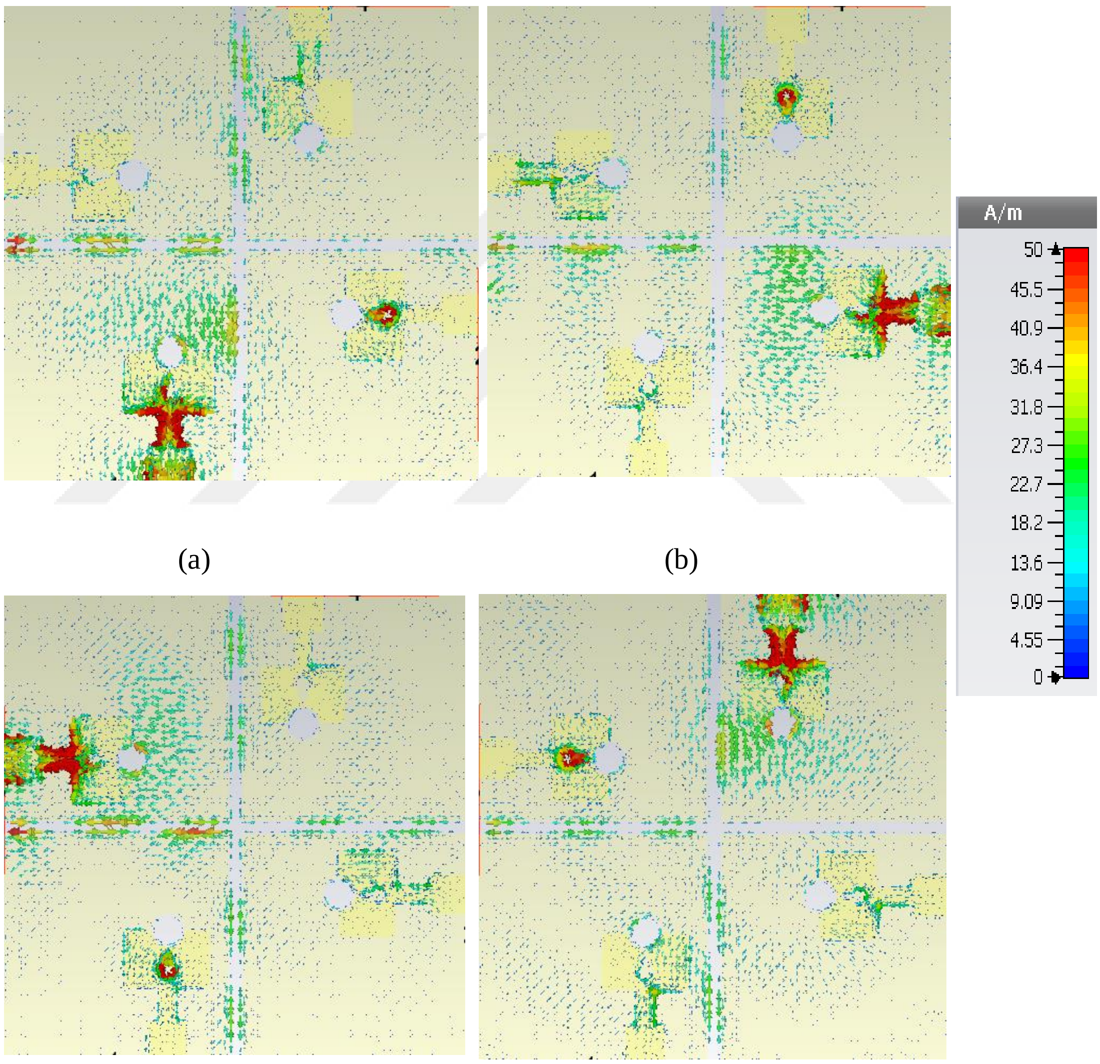

Figure 4.11. The surface current of a) the first port, b) the second port, c) the third port, d) the fourth port of the first design at 26 GHz

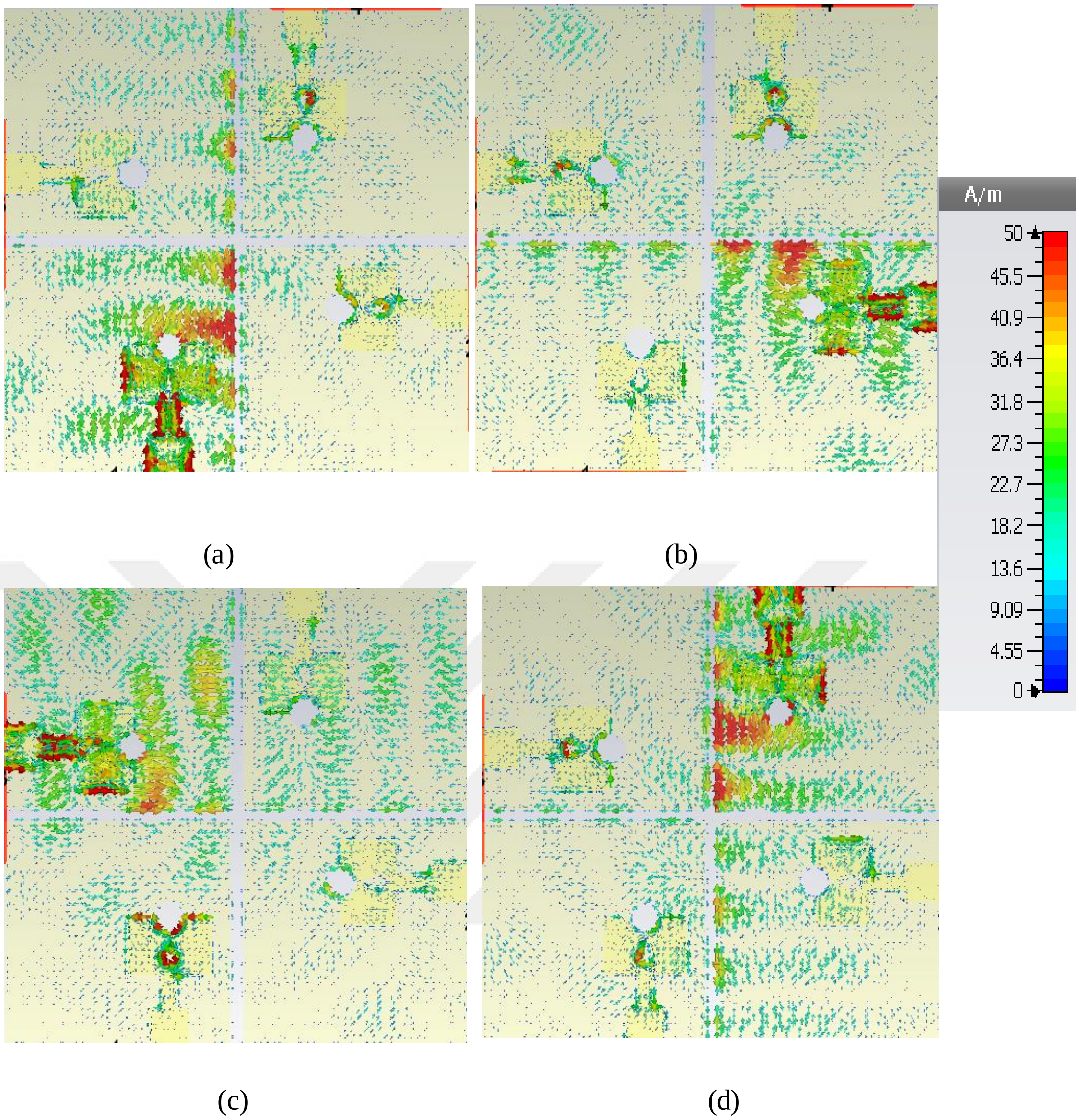

Figure 4.12. The surface current of a) the first port, b) the second port, c) the third port, d) the fourth port of the first design at 38 GHz

4.3. The result of the second MIMO Antenna

Figure 4.13 illustrates the return loss of each element. It can be noticed that they all propagate in the dual band and differ minimally regarding the return loss. The MIMO has the maximum return loss value of -18 dB and -33 dB at 28 GHz and 38 GHz, respectively. Also, the bandwidth is 5 GHz in the 28 GHz band and 5.5 GHz in the 38 GHz band.

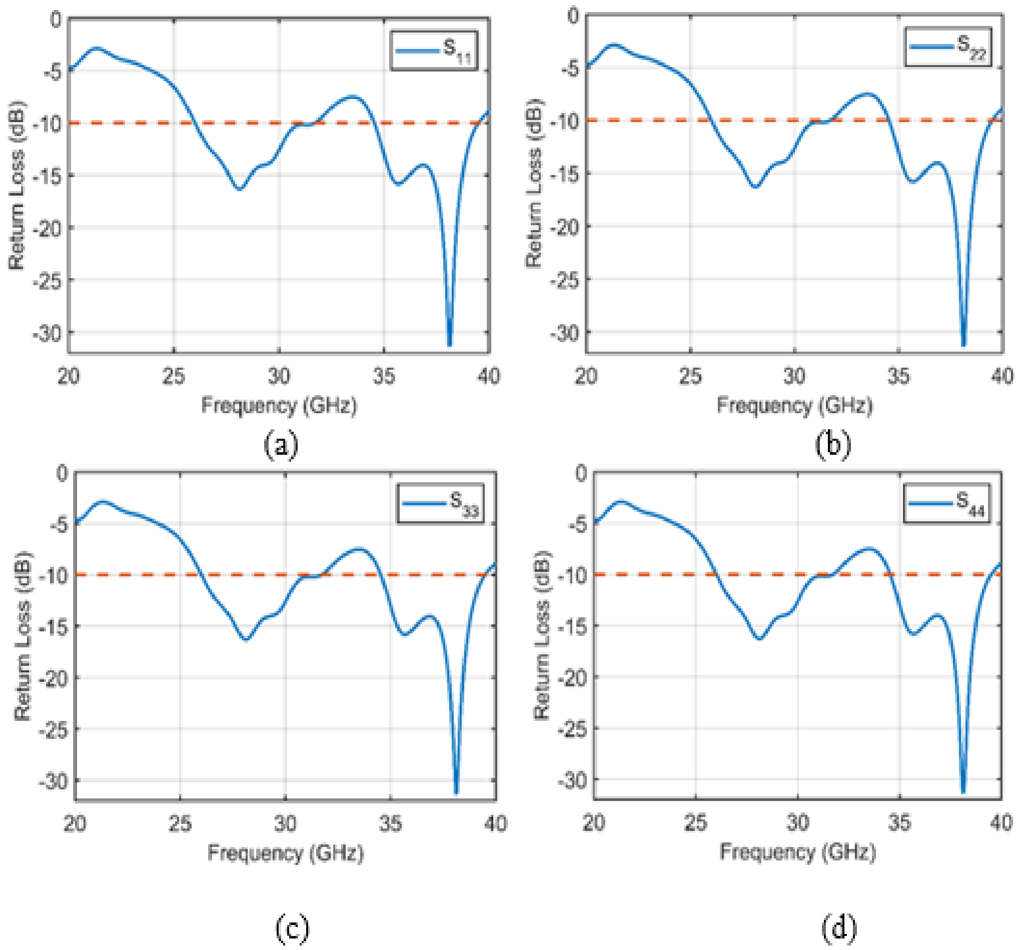

Figure 4.13. Each port's return loss of the second designed MIMO antenna

Figure 4.14 depicts the isolation between the radiating patches. From the diagram, it is clear that the average isolation at 28 GHz and 38 GHz is below -20 dB and -30 dB, respectively. This is due to the arrangement of the patches in a way that ensures low mutual coupling.

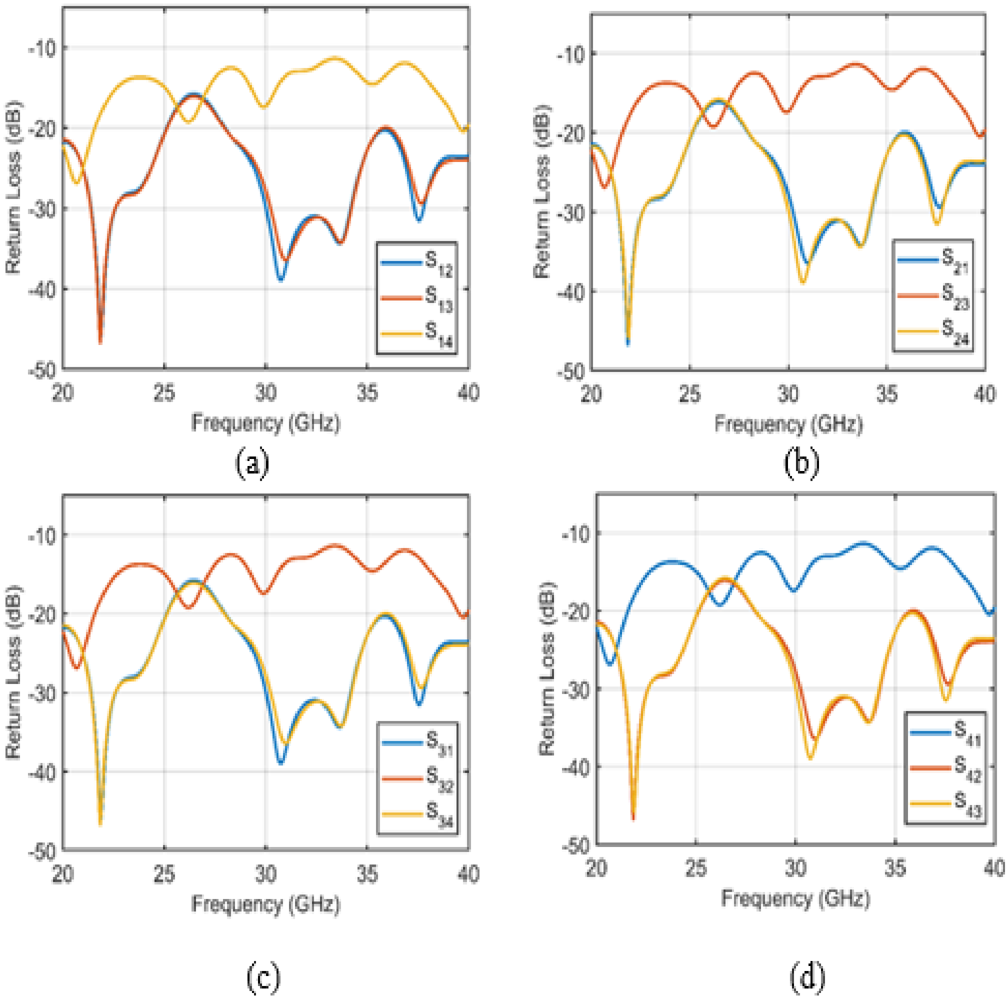

Figure 4.14. Port's isolation between each patch antenna of the second MIMO

Figure 4.15 illustrate the 3D simulated radiation patterns of the final MIMO antenna at 28 GHz for each antenna element are shown as a directional gain of the highest value of 10.6 dBi. Whereas Figure 4.16 displays the radiation pattern in the polar form and it shows that a) and d) have a main lobe magnitude of 10.1 dBi while b) and c) have a main lobe of 7.12 dBi and almost all elements show a directional pattern.

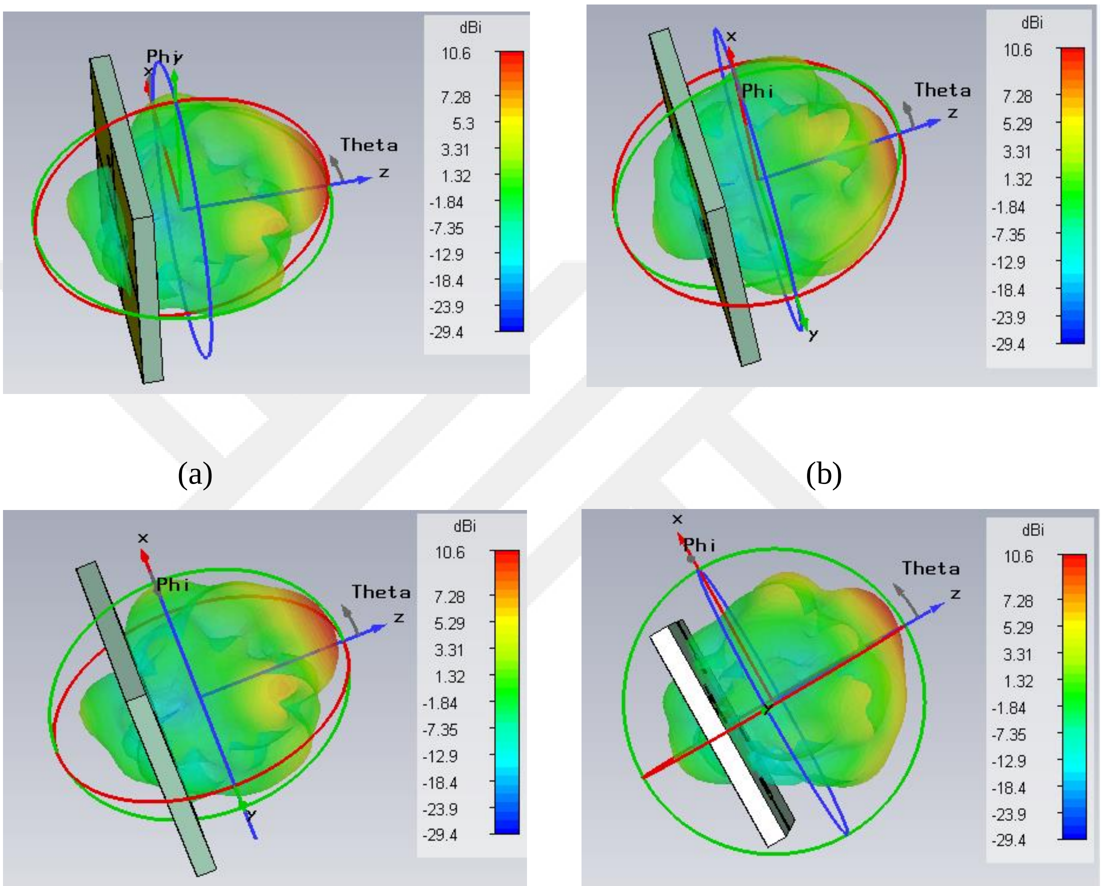

(a) (b)

(c) (d)

Figure 4.15. The 3D-dimensional radiation pattern at 28 GHz of a) the first port, b) the second port, c) the third port, d) the fourth port

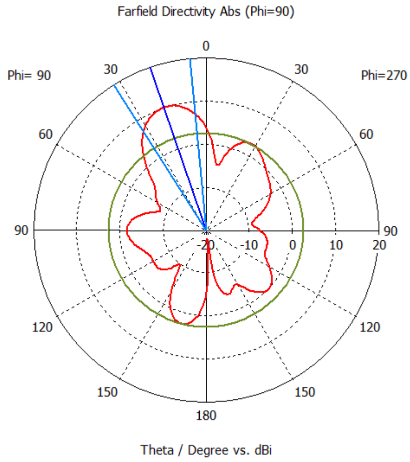

(a)

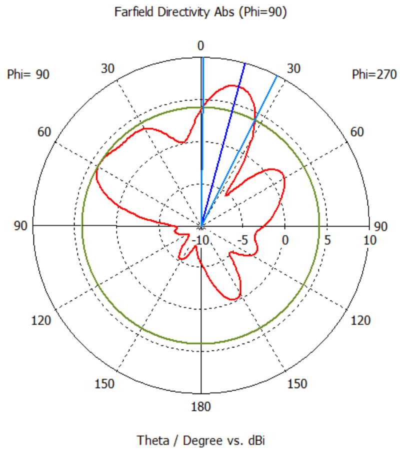

(b)

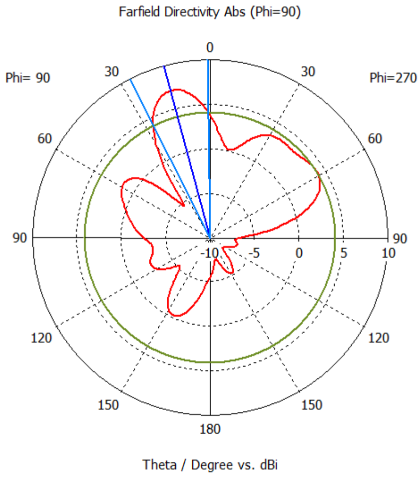

(c)

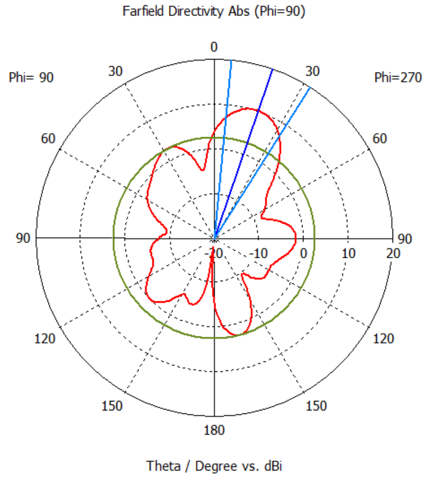

(d)

Figure 4.16. The polar radiation pattern at 28 GHz of a) the first port, b) the second port, c) the third port, d) the fourth port

At 38 GHz, the 3D simulated radiation patterns of the final MIMO antenna for each antenna element are shown as a directional gain of the highest value 6.65 dBi in Figure 4.17. Whereas Figure 4.18 displays the radiation pattern in the polar form and it shows that a) and d) have a main lobe magnitude of 4.03 dBi while b) and c) have a main lobe of 4.06 dBi and almost all elements show a semi-directional pattern.

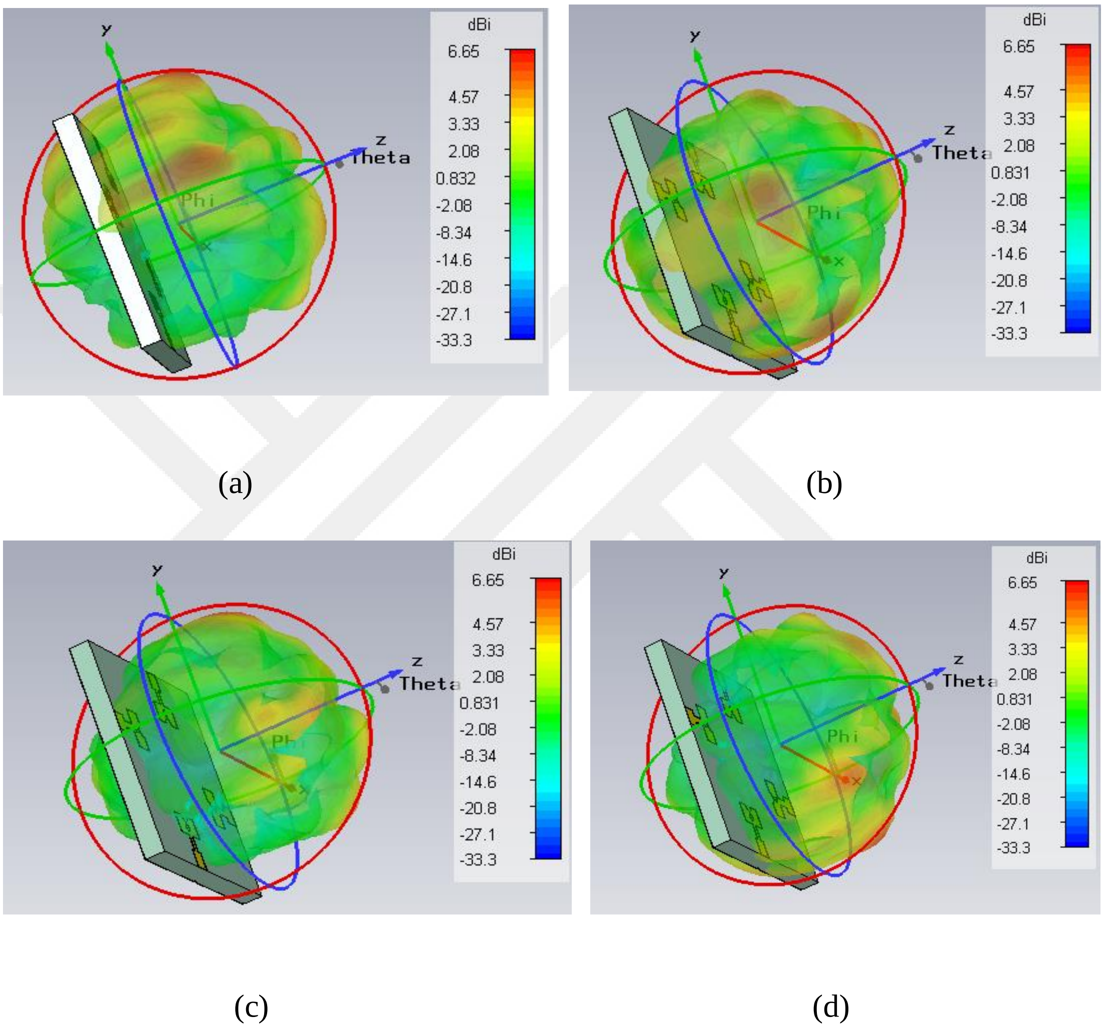

Figure 4.17. The 3D-dimensional radiation pattern at 38 GHz of a) the first port, b) the second port, c) the third port, d) the fourth port

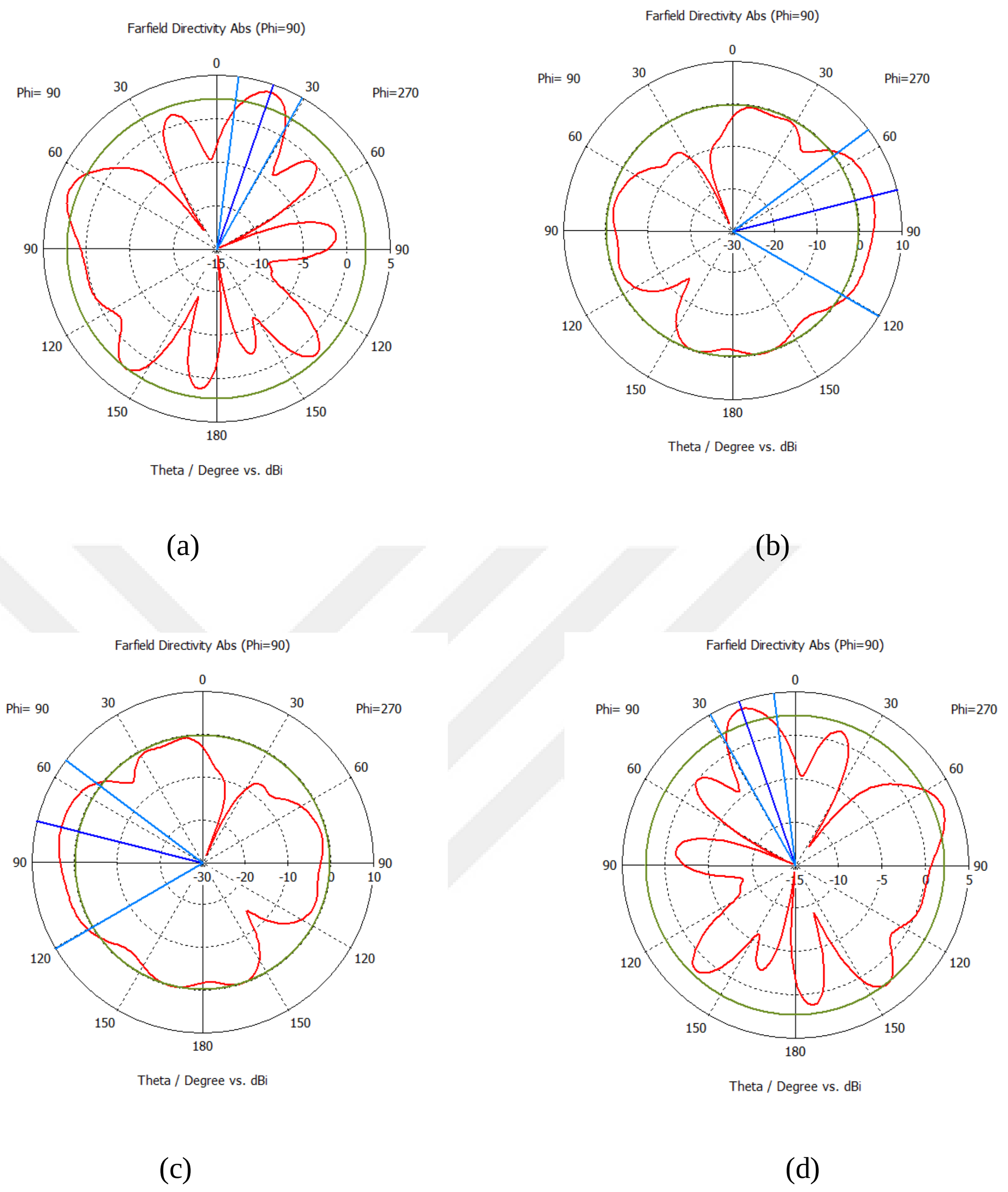

Figure 4.18. The polar radiation pattern at 38 GHz of a) the first port, b) the second port, c) the third port, d) the fourth port

Figure 4.19 display the efficiency for each element of the designed MIMO antenna. At 28 GHz the total efficiency is almost higher than 70% whereas at 38 GHz is almost 50% for all ports.

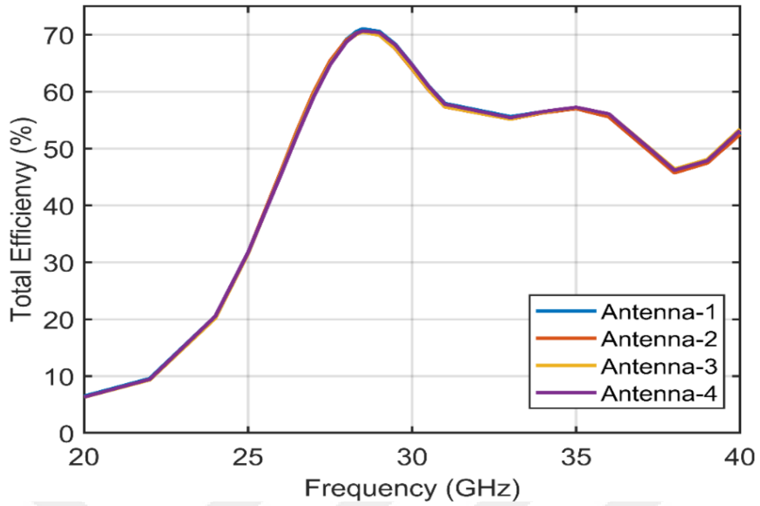

Figure 4.19. Antenna efficiency of each port of the second MIMO antenna.

Figure 4.20, displays the ECC of the second design between each port at 28 and 38 GHz. Additionally, Table 4.2 provides each ECC value between each port for both bands.

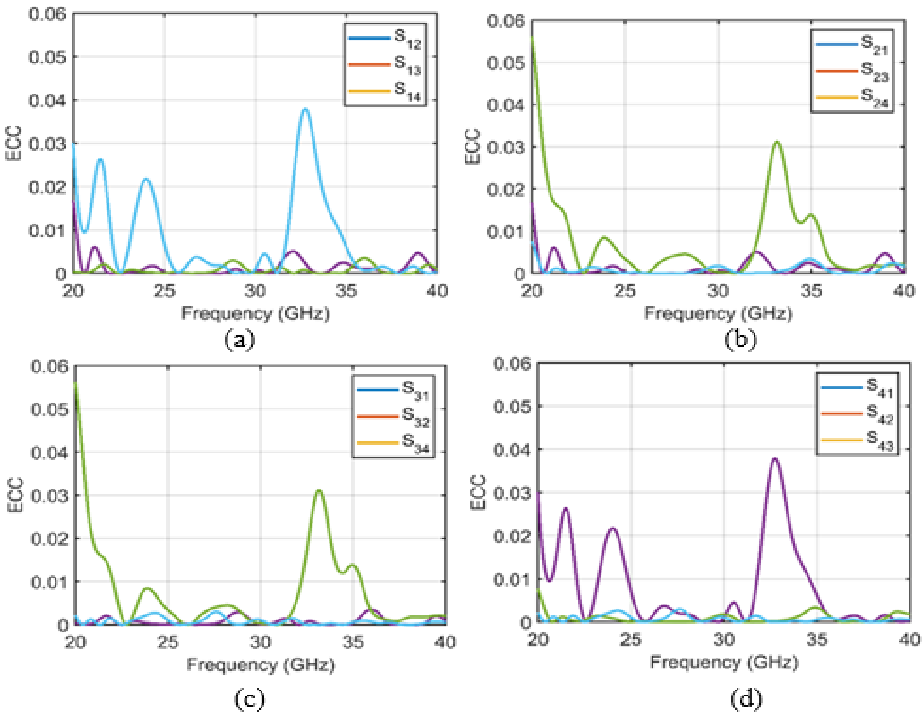

Figure 4.20. The performance of ECC for the second design

Table 4.2. Port's ECC value between each patch antenna of the second MIMO

ECC	28 GHz	38 GHz
S_{12} / S_{21}	0.00083	1×10^{-5}
S_{13} / S_{31}	0.00086	1×10^{-5}
S_{14} / S_{41}	5.574×10^{-6}	2.9×10^{-5}
S_{23} / S_{32}	5.566×10^{-6}	2.9×10^{-5}
S_{24} / S_{42}	0.00083	1×10^{-5}
S_{34} / S_{43}	0.00083	1×10^{-5}

Likewise, another key performance metric is diversity gain. In Figure 4.21, it can be seen that the DG is close to 10 dB at the desired frequency bands (28 and 38 GHz).

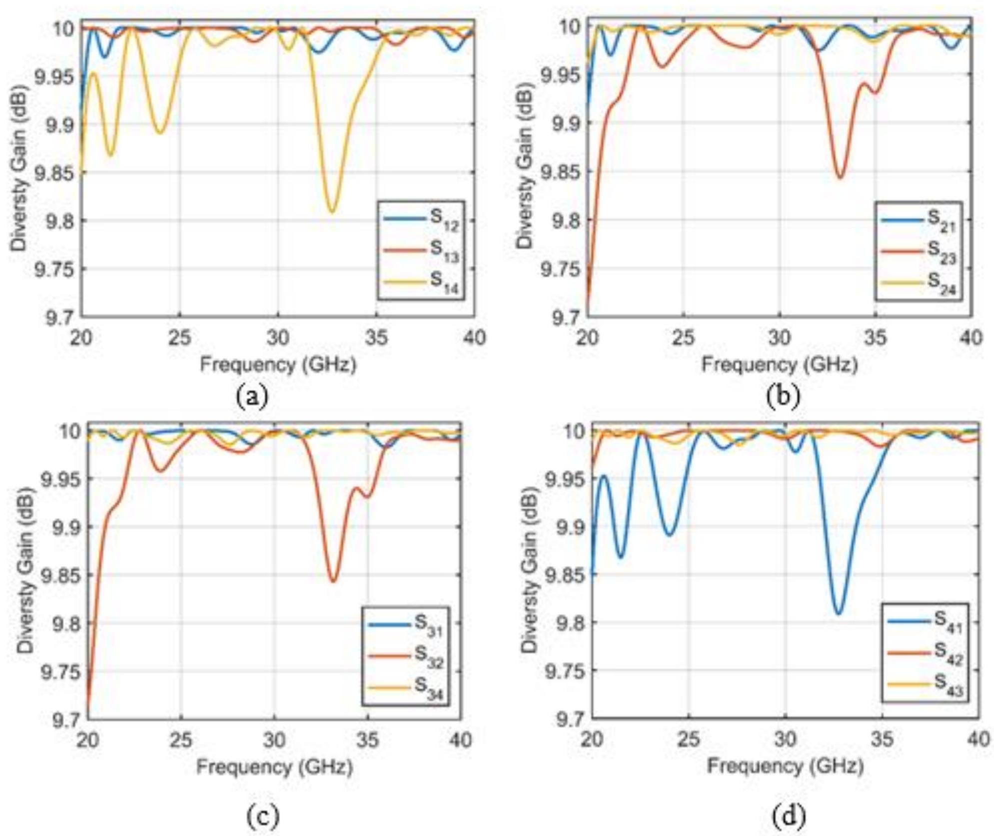

Figure 4.21. The performance of DG for the second designed

Fig. 4.22 and Fig. 4.23 show the distribution of the second designed MIMO antennal's surface current in each patch in the band of 28 GHz and 38 GHz, respectively. Accordingly, the current intensity across the connecting strips of the circular slots in the center of the patch is high. ThusThus, the slot and the connecting strips on the top of the feed contribute more to reaching the millimeter wave band. Moreover, the pattern of current distribution on the surface shows that the interference between the patches is negligible. Since each patch is arranged to be 90 degrees offset from the other.

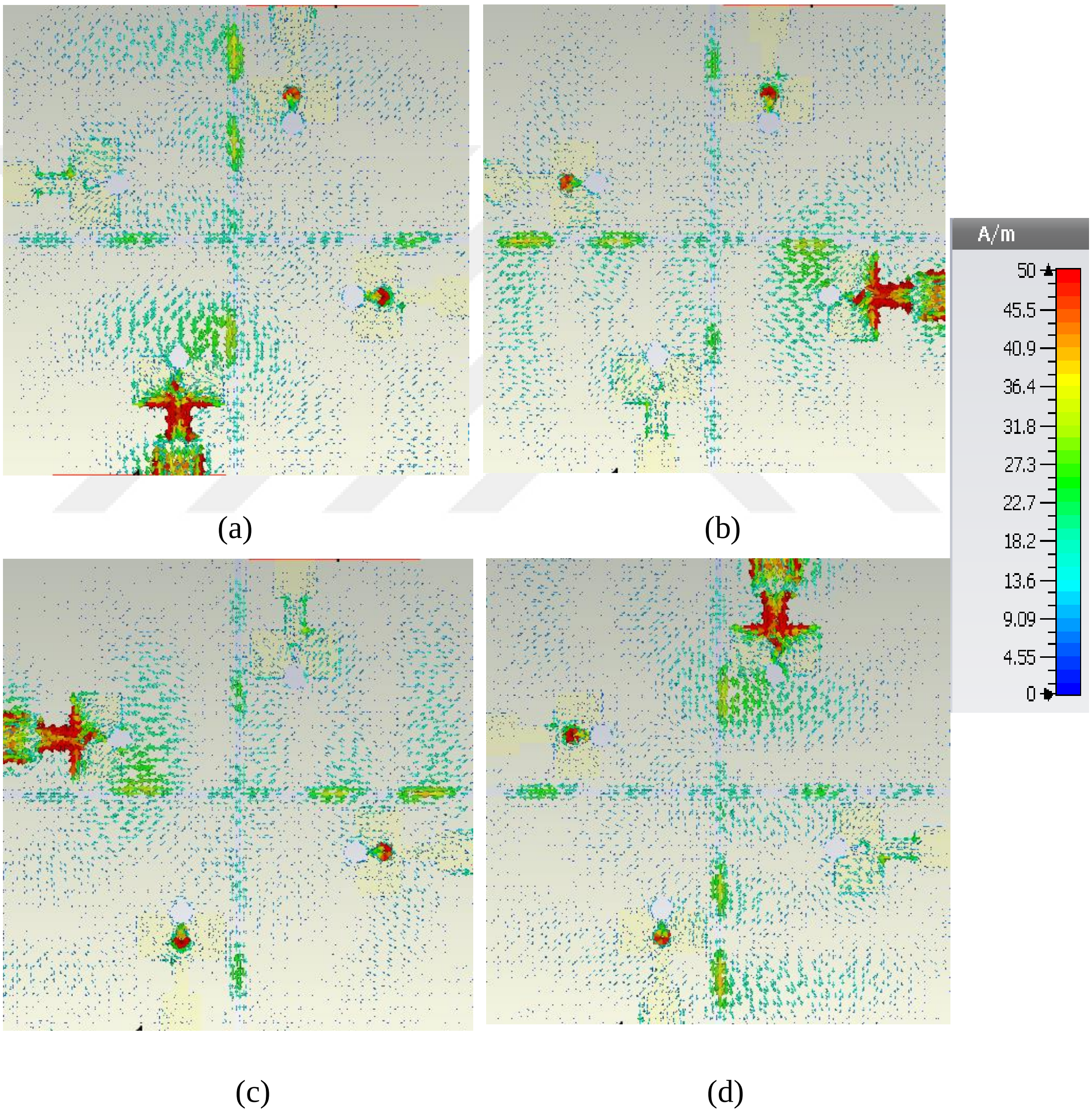

Figure 4.22. The surface current of a) the first port, b) the second port, c) the third port, d) the fourth port of the second design at 28 GHz

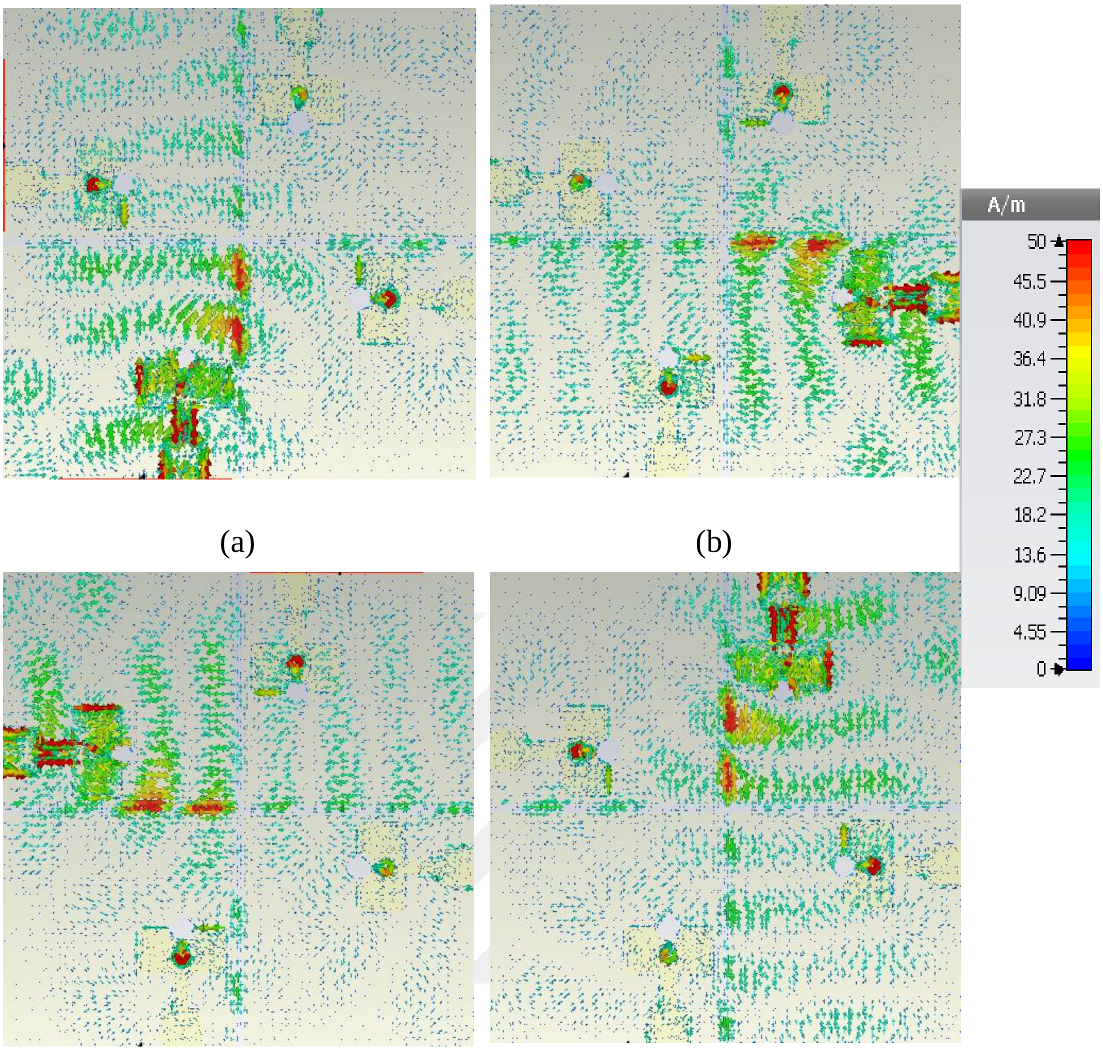

(a) (b)

(c) (d)

Figure 4.23. The surface current of a) the first port, b) the second port, c) the third port, d) the fourth port of the second design at 38 GHz

5. DISCUSSION

In this chapter, the results of the present study are discussed by comparing them with the thesis's initial objective, as well as with the antennas mentioned in the chapter "Literature Review" to determine whether the obtained antennas perform well.

5.1. Antenna Comparison

Comparing the proposed antenna to those from the literature review is presented in Table 5.1. The literature review reports various antenna designs operating at bands of 26 GHz, 28 GHz, and 38 GHz. It also includes a variety of designs that have a different number of elements such as 1 × 1, 2 × 2, 4 × 4, and 1 × 4. Furthermore, we have taken into account the sizes of other designs as it is one of our primary goals to design a 4x4 MIMO antenna that is small in size compared to other designs. As well as this, we have provided a detailed analysis of MIMO performance, including isolation, DG, and ECC between ports. Accordingly, the thesis presents MIMO antennas with significantly more performant than other antennas.

Table 5.1. Comparing the proposed antenna to other papers

Reference	Spectrum (GHz)	Bandwidth	Antenna Elements	Antenna size L x W (mm)	Return loss dB	Gain dBi	Efficiency %	Isolation dB	ECC
(Tu)	27.5-30 37-39	2.5 GHz 2 GHz	4 × 4	19.25 × 25	<-30	7 5	-	-	<0.004
(EL_Mashade and Hegazy)	27-28.3	1.3 GHz	1 × 4	31.677 × 7.07	-21.44	8.5	70	-	-
(Rahayu)	27.10-28.88	1.78 GHz	4 × 4	25 × 25	-32	8	70	-	-
(Hasan)	26.65- 29.2 37-39.05	2.55 GHz 2.05 GHz	2 × 2	14 ×26	-35	1.27 1.83	75	<-20	0.001
(Marzouk)	27-28.5 37-39	1.5 GHz 2 GHz	4 × 4	55 ×110	-21.57 -24.59	7.95 8	<70	-26	0.0000765
(Shuhrawardy)	26.6-39	12.4 GHz	4 × 4	30 × 25	<-15	5.2	70	<-20	0.002
(Sehrai)	23-40	17 GHz	4 × 4	80 × 80	-25	11	>70	>-20	<0.0014
(Khalid)	25.5–29.6	4.1 GHz	4 × 4	30 × 35	-23	7	<70	>-10	<0.01
(El Hadri)	27.5 - 28.35	0.85 GHz	2 × 2	12.8 × 26	-35	7	<60	>-30	.0000115
(Desai)	24.10- 27.18 33-40	3.08 GHz 7 GHz	4 × 4	24 × 20	-25	3	75	>-16	<0.1
(Hakim)	25-30 35-45	5 GHz 10 GHz	2 × 2	21.96 × 16.71	>-35	8.35 6.48	80	<-20	-
(Rahman)	27-29	2 GHz	4 × 4	30 × 30	-32	6	<70	>-15	<0.15
(Amrutha)	34-39	5 GHz	2 × 2	11 × 7.5	-25	3.65	-	<-22	<0.01
(Sehrai)	36.83-40	3.17 GHz	4 × 4	23.7 × 8.8	-25	6.5	<80	<-30	<0.5
(Saleem)	27.5-30.25 37-40	2.75 GHz 3 GHz	4 × 4	14 × 14	<-28 <-17	7.09 3.43	55	<-24 <-17	0.014
(Ghosh and Swati)	27.8- 28.8	1 GHz	2 × 2	40 × 18.607	-22	10	-	<-25	<0.001

(Awan)	27–30	3 GHz	1× 1	15 × 15	-22	5.69	-	-	-
(Raheel)	27.6–28.6 37.4–38.6	1 GHz 1 GHz	4 × 4	20 × 24	-18 -20	7.1 7.9	<85	<-25	<0.001
(Kamal)	27.5-29	1.5 GHz	4 × 4	30 × 30	-35	5.5	<75	>-18	<0.15
(Sabek)	25.9 - 30.4 36.4 - 40.2	5.4 GHz 3.8 GHz	1× 1	12×12	<-20	4.5	80	-	-
(Desai and Neelgar)	24.2–26.59	2.39 GHz	4 × 4	15 × 15	-13.9	5.38	<80	<-23	<0.005
(El Hadri)	34-45	11 GHz	2 × 2	12.8 × 26	-33	7.12	70	>-25	>0.0002
(Chaudhary and Kansal)	27.9-28.45 37.5-38.5	0.55 GHz 1 GHz	2 × 2	10 × 17	-25 -15	7.46 8.56	77	-23.3 -21.4	0.0023
(Manirathnam)	27.25-28.73	1.48 GHz	2 × 2	22 × 12	-35	6.82	-	<-25	<0.0002
Proposed MIMO 1	23-28.5 35-39.5	5.5 GHz 4.5 GHz	4 × 4	18 × 18	-26 -41	9.14 6.71	>60 50	-20 -30	<0.000001
Proposed MIMO 2	26-31 34.5-40	5 GHz 5.5 GHz	4 × 4	18 × 18	-18 -33	10.6 6.65	>70 >50	-20 -30	<0.000001

6. CONCLUSION

The presented thesis sought the design and optimization of two structures of 4 × 4 MIMO antenna operating on different mm-wave bands in a dual-band mode. This was initiated by analyzing the key features of a typical antenna and its parameters which are used to identify its purpose and efficiency. This was followed by an exploration of other designs of antennas with similar characteristics to the one presented.

In the proposed design, initially, a single antenna with an FR-4 dielectric substrate and a rectangular patch antenna was created as part of the proposed design of four elements. After that, the antenna’s parameters have gone under numerous procedures, which were continuously generated with the simulations in the software CST, aiming at identifying and optimizing the antenna's strengths and weaknesses.

These procedures included the addition and constant modification of up to four slots and one slot on the patch antenna and the ground, respectively. After reaching the last design of the antenna with the most satisfactory characteristics, the 5G MIMO antenna was constructed by implementing four identical elements arranged circularly, in which they have minimal interference with each other.

The initial design of the MIMO antenna was supporting the Europe standard (24.25 to 27.5 GHz). However, it has gone through different procedures to comply with the U.S. standard (26.5 to 29.5 GHz).

Our results of the first design antenna operates from 23 to 28.5 GHz and from 35 to 39.5 GHz. At 26 GHz, it features a gain of 9.86 dBi with a radiation efficiency of more than 60%. While at 38 GHz, it features a gain of 6.71 dBi with a radiation efficiency of more than 50%.

Whereas the second design operates from 26 to 31 GHz and from 34.5 to 40 GHz. It also features a high gain of 10.6 and 6.65 dBi at 28 and 38 GHz, respectively. The radiation efficiency is more than 70% at 28 GHz and 50% at 38 GHz.

For both designs, we figured out that the average isolation is -20 dB at the first band and -30 dB at the second band, according to simulation results. As well, the DG is nearly 10 dB and the ECC is less than 1×10^{-6}, providing excellent performance compared to previous antenna designs.

6.1. Future Work

In this part, we fabricated the single antenna as shown in figure 6.1, and the first MIMO antenna design as shown in Figure 6.2. Due to the high frequencies of the designed antennas, we faced difficulties in the measurement. Furthermore, after doing the measurement we figure out that there was an error in the type of the connector and we were supposed to use SMP instead of SMA. Since SMA provides a performance that can reach up to 25 GHz while SMP can reach up to 40 GHz.

For future work measure the designed antennas to compare the measurement results with the simulation results. Also, Simulate the antenna designs on different simulation programs.

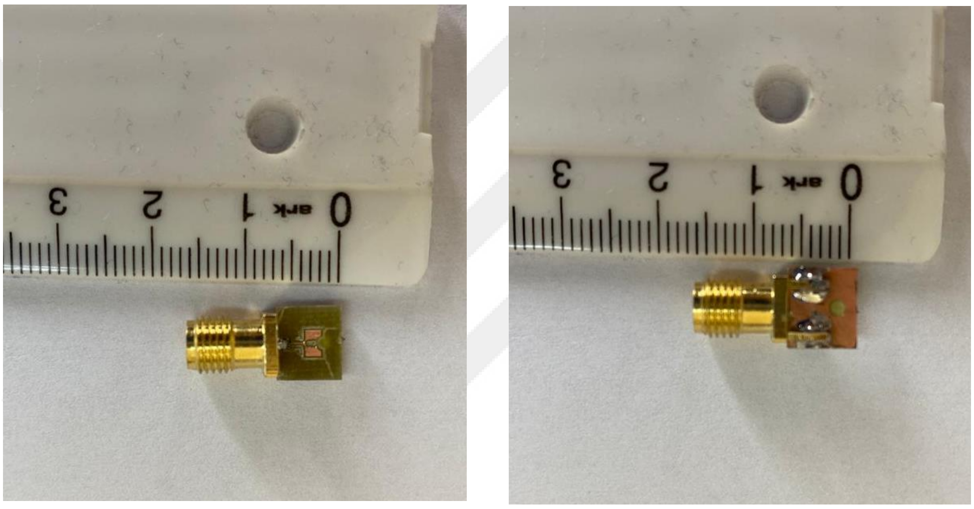

Figure 6.1. a) front, b) back side of the fabricated single antenna

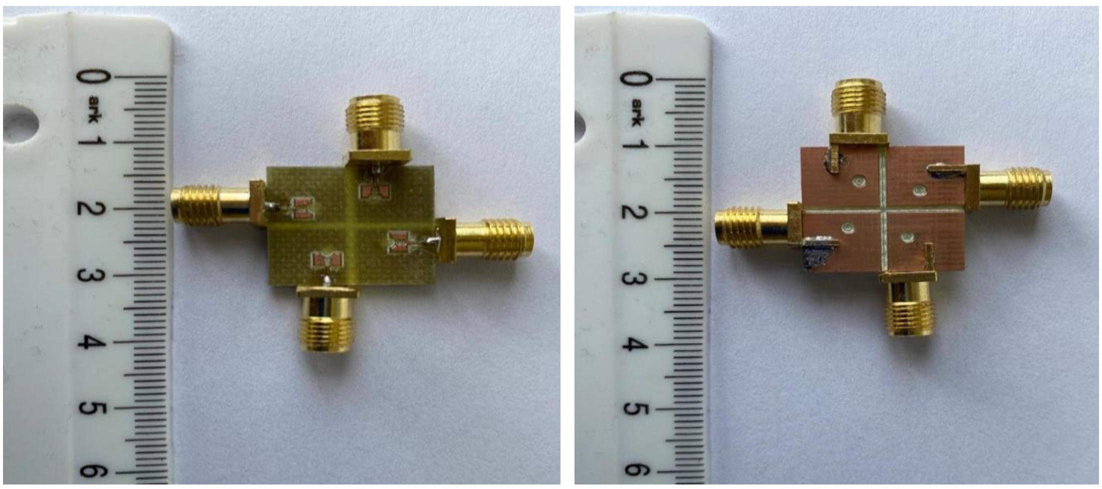

Figure 6.2. a) front, b) back side of the fabricated first MIMO antenna

REFERENCES

Al-Falahy, N., and Alani, O. Y. (2019). Millimetre wave frequency band as a candidate spectrum for 5G network architecture: A survey. Physical Communication, 32, 120-144.

Adachi, F. (2002, October). Evolution towards broadband wireless systems. In The 5th International Symposium on Wireless Personal Multimedia Communications (Vol. 1, pp. 19-26). IEEE.

Amrutha, P., Prasad, K. L. V., and Kumar, S. (2021). Highly Isolated Fork-Shaped MIMO Antenna for 5G Application. In 2021 Asian Conference on Innovation in Technology (ASIANCON) (pp. 1-4). 27-29 August, IEEE, PUNE, India.

Ang, B.K. Chung, B.K. (2007). A wideband e-Shaped Microstrip Patch Antenna for 5–6 GHz Wireless Communications. *Progress In Electromagnetics Research*, PIER 75, 397–407.

Awan, W. A., Naqvi, S. I., Naqvi, A. H., Abbas, S. M., Zaidi, A., and Hussain, N. (2021). Design and Characterization of Wideband Printed Antenna Based on DGS for 28 GHz 5G Applications. Journal of Electromagnetic Engineering and Science, 21(3), 177-183.

Aironet, C. (2007). Antenna Patterns and Their Meaning.

Balanis, C.A. (2005). Antenna Theory: Analysis and Design: Willey-Inter Science.

Balanis, C. A. (2012). Advanced Engineering Electromagnetics: Wiley.

Chaudhary, S., and Kansal, A. (2022). Compact high gain 28, 38 GHz antenna for 5G communication. International Journal of Electronics, 1-21.

Cronin, T. W. (2018). A different view: sensory drive in the polarized-light realm. Current Zoology, 64(4), 513-523.

Connector supplier, (2022).What are SMA Connectors?, https://connectorsupplier.com/meet-the-connector-sma-connectors , (Accessed 1 Octuber 2022).

Desai, A., Bui, C. D., Patel, J., Upadhyaya, T., Byun, G., and Nguyen, T. K. (2020). Compact wideband four element optically transparent MIMO antenna for mm-wave 5G applications. IEEE Access, 8, 194206-194217.

Desai, P. K., and Neelgar, B. (2021, December). Design of Compact 4× 4 MIMO Antenna with DGS Structure for 5G mmWave Communication. In 2021 International Conference on Circuits, Controls and Communications (CCUBE) (pp. 1-6). 23-24 December, IEEE, Bangalore, India.

El_Mashade, M. B., and Hegazy, E. A. (2018). Design and analysis of 28GHz rectangular microstrip patch array antenna. WSEAS Transactions on Communications, 17(1),1- 9.

El Hadri, D., Zakriti, A., Zugari, A., El Ouahabi, M., and El Aoufi, J. (2020). High isolation and ideal correlation using spatial diversity in a compact MIMO antenna for fifth-generation applications. International Journal of Antennas and Propagation, 2020(1),1-10.

El Hadri, D., Zugari, A., and Zakriti, A. (2022). Extra Wide Band MIMO Antenna with High Isolation and Low Correlation at 38 GHz mm-Wave Frequency Band for 5G Applications. In E3S Web of Conferences (Vol. 351, p. 01076). EDP Sciences.

Everything RF, (2019). What is MIMO Technology?, https://www.everything rf.com/community/what-is-MIMO-technology, (Accessed 1 November 2022).

Embedded Computıng Desıgn, (2021) Will 5G mmWave See a Large-Scale Rollout?, https://embeddedcomputing.com/application/networking-5g/5g/will-5g mmwave-see-a-large-scale-rollout,(Accessed 1 November 2022).

Ghosh, S., and Swati, M. V. (2021). A compact mm-wave MIMO antenna array. 2021 Asian Conference on Innovation in Technology (ASIANCON) (pp. 1-4). 27-29 August, IEEE, PUNE, India.

Microwave Journal, (2019). Global 5g Rush But No Global 5g Handsets, https://www.microwavejournal.com/articles/31757-global-5g-rush but-no-global-5g-handsets. (Accessed 1 November 2022).

Hasan, M. N., Bashir, S., and Chu, S. (2019). Dual band omnidirectional millimeter wave antenna for 5G communications. Journal of Electromagnetic Waves and Applications, 33(12), 1581-1590.

Hakim, M. L., Uddin, M. J., and Hoque, M. J. (2020, June). 28/38 GHz Dual-Band Microstrip Patch Antenna with DGS and Stub-Slot Configurations and Its 2× 2 MIMO Antenna Design for 5G Wireless Communication. 2020 IEEE Region 10 Symposium (TENSYMP) (pp. 56-59). 05-07 Jun, IEEE, Dhaka, Bangladesh.

Harrington, R. F. (1960). Effect of Antenna Size on Gain, Bandwidth, and Efficiency. Journal of research of the National Bureau of Standards, 64(1), 1-12.

Hiçdurmaz, B., and Gümüş, Ö. F. (2019). Design and analysis of 28 GHz microstrip patch antenna for different type FR4 claddings. Uludağ Üniversitesi Mühendislik Fakültesi Dergisi, 24(2), 265-288.

Joshi, M. P., and Gond, V. J. (2017, May). Microstrip patch antennas for wireless communication: A review. In 2017 International Conference on Trends in Electronics and Informatics (ICEI) (pp. 96-99). IEEE.

Khalid, M., Iffat Naqvi, S., Hussain, N., Rahman, M., Mirjavadi, S. S., Khan, M. J., and Amin, Y. (2020). 4-Port MIMO antenna with defected ground structure for 5G millimeter wave applications. Electronics, 9(1),1-13.

Kamal, M. M., Yang, S., Ren, X. C., Altaf, A., Kiani, S. H., Anjum, M. R., and Saeed, S. I. (2021).Infinity shell shaped MIMO antenna array for mm-wave 5G applications. Electronics, 10(2), 1-12.

Khan, R. (2017). Review Paper of Antenna. *International Journal of Engineering Research & Technology (IJERT)*, 5(23).

Khattak, M. I., Sohail, A., Khan, U., Barki, Z., and Witjaksono, G. (2019). Elliptical slot circular patch antenna array with dual band behaviour for future 5G mobile communication networks. Progress In Electromagnetics Research C, 89, 133-147.

Küpeli, M. (2017). *Çift Bant Mikroşerit GPS Anten Analizi ve Tasarımı*. Basılmamış Yüksek Lisans Tezi Hacettepe Üniversitesi, Lisansüstü Elektrik-Elektronik Mühendisliği Anabilim Dalı.

Lawrence, N. P., Ng, B. W. H., Hansen, H. J., and Abbott, D. (2017). 5G terrestrial networks: Mobility and coverage—Solution in three dimensions. IEEE Access, 5, 8064-8093.

Marzouk, H. M., Ahmed, M. I., and Shaalan, A. H. A. (2019). Novel dual-band 28/38 GHz MIMO antennas for 5G mobile applications. Progress In Electromagnetics Research C, 93, 103-117.

Manirathnam, C., Ghosh, S., and Swati, M. V. (2022). A Compact, Two-Port MIMO Antenna for mm-wave 5G Application. In 2022 IEEE 11th International Conference on Communication Systems and Network Technologies (CSNT) (pp. 22-25). 23-24 April, IEEE, Indore, India.

Osseiran, A., Boccardi, F., Braun, V., Kusume, K., Marsch, P., Maternia, M., ... & Fallgren, M. (2014). Scenarios for 5G mobile and wireless communications: the vision of the METIS project. IEEE communications magazine, 52(5), 26-35.

Ojaroudiparchin, N., Shen, M., and Pedersen, G. F. (2015, November). A 28 GHz FR-4 compatible phased array antenna for 5G mobile phone applications. In 2015 International symposium on Antennas and propagation (ISAP) (pp. 1-4). IEEE.

Rahayu, Y., Afif, L., Radhelan, M. R., Yasri, I., and Candra, F. (2018). Design of 28 GHz microstrip MIMO antennas for future 5G applications, 22(3), 149-154.

Rahman, M., NagshvarianJahromi, M., Mirjavadi, S. S., and Hamouda, A. M. (2019). Compact UWB band-notched antenna with integrated bluetooth for personal wireless communication and UWB applications. Electronics, 8(2).

Rahman, S., Ren, X. C., Altaf, A., Irfan, M., Abdullah, M., Muhammad, F., and AlKahtani, F. S. (2020). Nature inspired MIMO antenna system for future mmWave technologies. Micromachines, 11(12), 1-11.

Raheel, K., Altaf, A., Waheed, A., Kiani, S. H., Sehrai, D. A., Tubbal, F., and Raad, R. (2021). E-shaped H-slotted dual band mmWave antenna for 5G technology. Electronics, 10(9), 1-10.

Rangan, S., Rappaport, T. S., and Erkip, E. (2014). Millimeter-wave cellular wireless networks: Potentials and challenges. Proceedings of the IEEE, 102(3), 366-385.

Rappaport, T. S., Sun, S., Mayzus, R., Zhao, H., Azar, Y., Wang, K., and Gutierrez, F. (2013). Millimeter wave mobile communications for 5G cellular: It will work. IEEE access, 1, 335-349.

Rescale, (2022). https://rescale.com/documentation/software-examples-a-e/cst-examples/, (Accessed 1 October 2022).

Shuhrawardy, M., Chowdhury, M. H. M., and Azim, R. (2019). A four-element compact wideband MIMO antenna for 5G applications. In 2019 International Conference on Electrical, Computer and Communication Engineering (ECCE) (pp. 1-5). 07-09 February, IEEE, Cox'sBazar, Bangladesh.

Sehrai, D. A., Abdullah, M., Altaf, A., Kiani, S. H., Muhammad, F., Tufail, M., and Rahman, S. (2020). A novel high gain wideband MIMO antenna for 5G millimeter wave applications. Electronics, 9(6), 1-13.

Sehrai, D. A., Asif, M., Shoaib, N., Ibrar, M., Jan, S., Alibakhshikenari, M., and Limiti, E. (2021). Compact quad-element high-isolation wide and MIMO antenna for mm-wave applications. Electronics, 10(11), 1-10.

Saleem, S., Kumari, S., Yadav, D., and Bhatnagar, D. (2021). Compact millimeter-wave MIMO (multiple-input multiple-output) antenna for 5G Applications. In 2021 IEEE Indian Conference on Antennas and Propagation (InCAP) (pp. 1035-1038). 13-16 December, IEEE, Jaipur, Rajasthan, India.

Sabek, A. R., Ibrahim, A. A., & Ali, W. A. (2021). Dual-band millimeter wave microstrip patch antenna with stubresonators for 28/38 GHz applications. In Journal of Physics: Conference Series, 2128(1).

Sharawi, M. S. (2013). Printed multi-band MIMO antenna systems and their performance metrics [wireless corner]. IEEE Antennas and propagation Magazine, 55(5), 218-232.

Surantha, N., Sutisna, N., Nagao, Y., and Ochi, H. (2017, September). SoC design with HW/SW co-design methodology for wireless communication system. In 2017 17th International Symposium on Communications and Information Technologies (ISCIT) (pp. 1-6). IEEE.

Tu, D. T. T., Thang, N. G., Ngoc, N. T., Phuong, N. T. B., and Van Yem, V. (2017). 28/38 GHz dual-band MIMO antenna with low mutual coupling using novel round patch EBG cell for 5G applications. In 2017 International Conference on Advanced Technologies for Communications (ATC) (pp. 64-69). 18-20 October, EEE, Quy Nhon, Vietnam.

5G spectrum bands explained. (2020), https://www.nokia.com/networks/insights/spectrum-bands-5g-world/, (Accessed 9 November 2022).

5G Frequency Bands, 2022, https://halberdbastion.com/technology/cellular/5g-nr/5g-frequency-bands, (Accessed 9 November 2022).

Zakariyya, O. S., Sadiq, B. O., Abdulrahman, O. A., and Salami, A. F. (2016). Modified edge fed Sierpinski carpet miniaturized microstrip Patch antenna. Nigerian Journal of Technology, 35(3), 637-641.

CURRICULUM VITAE

My name is Nermin Hamdan, I hold a bachelor's degree in computer and communication engineering from Al-Azhar University in Palestine with a degree of excellence. In 2019 I worked at the engineering department at Al-Azhar University as a teacher's Assistant. In 2020 I got accepted into the turkey scholarship to pursue my master's degree in communication engineering at Ondokuz Mayıs University, Institute of Science and Technology, Department of Electrical and Electronics Engineering.

Contact Information :

ORCID ID : 0000-0002-5347-2832

Publications :

1. Hamdan, N., & Kurnaz, C. (2022, July). Four Element MIMO Antenna Design at 28 GHz for 5G Wireless Communication Systems. In 2022 45th International Conference on Telecommunications and Signal Processing (TSP) (pp. 183-186). IEEE.